DUAL RECIPROCITY BOUNDARY ELEMENT ANALYSIS OF HELMHOLTZ EQUATIONS WITH VARIABLE COEFFICIENTS

Under the Guidance of
Prof. Arup Guha Niyogi

Arnab Samanta
Master of Civil Engineering (Structural Engineering)
Class Roll- 002010402030
Examination Roll- M4CIV22030
Registration Number- 127247 of 2014-15
Department of Civil Engineering
Jadavpur University
Kolkata-700032

Session 2021-2022

DEPARTMENT OF CIVIL ENGINEERING
FACULTY OF ENGINEERING AND TECHNOLOGY
JADAVPUR UNIVERSITY
KOLKATA-700032

CERTIFICATE OF RECOMMENDATION

This is to certify that the thesis entitled **"DUAL RECIPROCITY BOUNDARY ELEMENT ANALYSIS OF HELMHOLTZ EQUATIONS WITH VARIABLE COEFFICIENTS"** submitted by **Arnab Samanta**, class roll: 002010402030, exam roll: M4CIV22030 and registration number: 127247 of 2014-15, in partial fulfilment of the requirements for the award of Master of Engineering degree in Civil Engineering with specialization in "Structural Engineering" at Jadavpur University, Kolkata is an authentic work carried out by him under my supervision and guidance.

I hereby recommend that the thesis be accepted in partial fulfilment of the requirements for awarding the degree of **"Master of Engineering in Civil Engineering (Structural Engineering)"**

Dr. Arup Guha Niyogi
Professor
Department of Civil Engineering
Jadavpur University

Countersigned by

Head of the Department
Department of Civil
Engineering
Jadavpur University

Dean
Faculty of Engineering and Technology
Jadavpur University

DEPARTMENT OF CIVIL ENGINEERING
FACULTY OF ENGINEERING AND TECHNOLOGY
JADAVPUR UNIVERSITY
KOLKATA-700032

CERTIFICATE OF APPROVAL

This thesis paper is hereby approved as a credible study of an engineering subject carried out and presented in a manner satisfactorily to warrant its acceptance as a pre-requisite for the degree for which it has been submitted. It is understood that, by this approval the undersigned do not necessarily endorse or approve any statement made, opinion expressed or conclusion drawn therein but approved the thesis paper only for the purpose for which it is submitted.

Committee of Thesis Paper Examiners

Signature of Examiner

Signature of the Examiner

DECLARATION

I, Arnab Samanta, Mater of Engineering (Structural Engineering), Jadavpur University, Faculty of Engineering and Technology, hereby declare that the work being presented in the thesis work entitled, **“DUAL RECIPROCITY BOUNDARY ELEMENT ANALYSIS OF HELMHOLTZ EQUATIONS WITH VARIABLE COEFFICIENTS”**, is authentic record of work has been carried out at the Department of Civil Engineering, Jadavpur University, Kolkata under Dr. Arup Guha Niyogi, Professor of Department of Civil Engineering, Jadavpur University. The work contained in the thesis has not yet been submitted in part or full to any other university or institution or professional body for award of any degree or diploma or any fellowship.

Arnab Samanta

Class Roll: 002010402030

Exam Roll: M4CIV22030

Reg. No.: 127247 of 2014-15

Place: Kolkata

Date:

ACKNOWLEDGEMENT

I express my deep sense of respect and gratitude to Dr. Arup Guha Niyogi, Professor of Department of Civil Engineering, Jadavpur University under whose supervision the work has been done. He has taken the strain of giving valuable suggestions to me from time to time. It is his never-ending enthusiasm and constant urge for excellence that has given me to bring this thesis work to completion.

I extend my thanks to all the faculty members of Department of Civil Engineering, Jadavpur University for providing their moral support, encouragement, and the necessary infrastructure for the work. I also acknowledgement the cooperation and assistance provided by my friends during this period.

Arnab Samanta

Class- MCE-II

Class Roll: 002010402030

Exam Roll: M4CIV22030

Reg. No.: 127247 of 2014-15

Table of Contents

List of Figures

List of Tables

List of Symbols

$\varphi(\mathrm{x},\mathrm{y})$ = Potential at point (x, y)

$\frac{\partial\varphi}{\partial n}$ = Flux

$n_{x,}\ n_y$ =Unit normal vector of X and Y components

R= Two-dimensional domain of interest

$P(\xi, \eta)$ = Point source at point (ξ, η)

$Q(x, y)$ = Field point located at (x, y)

ρ = Radius

$\Phi(x, y; \xi, \eta)$ = Fundamental solution for Laplace equation

$\lambda(\xi, \eta)$ = Free term coefficient

$C^{(k)}$ = ‘k’th boundary element

$\alpha(x, y)$ = Constant of Helmholtz equation

$g(x, y)$ = Constant of Helmholtz equation

$\rho(x, y; a, b)$= Assumed radial basis function

$\delta^{(nm)}$ = Dirac delta function

N= Number of boundary nodes

L= Number of interior nodes

P, P_o = instantaneous and ambient pressures, respectively

ρ ,ρ_o = instantaneous and ambient mass densities respectively

B= adiabatic bulk modulus

s= condensation

ξ_{ai} = particle displacement from its equilibrium position.

$\vec{u}_a$ =Fluid flow velocity

k= wave number

Abstract of the thesis

Practical engineering problems have complex domains and boundary conditions which make them difficult to solve using analytical methods. Hence, such engineering problems are often solved numerically to a desired level of accuracy. There are several approximation methods for making numeric solutions, of which the boundary element method (BEM) has been adopted in my thesis work where problem's dimensionality is shortened by one. Three-dimensional elements can be modelled with two-dimensional elements and similarly two-dimensional domains can be modelled with line elements. BEM requires less processing time and storage space than domain approaches such as finite element or finite difference methods. For this reason, boundary element method has been preferred here. Initially, the formulation of boundary element is employed to Laplace type equation. Later, we attempted Helmholtz type equations. Since Helmholtz equation involves non-homogenous terms, therefore to solve Helmholtz equations we have to go for domain integration technique. However, domain integration technique lacks the flavor of a true "boundary-only" solution. By adopting dual reciprocity boundary element method (DRBEM) this lacuna can be overcome. In my thesis work by using dual reciprocity boundary element method Helmholtz type equation is solved. For practical engineering problem numerical problem on acoustics is solved. A FORTRAN 77 program is developed for the present purpose with constant elements. This eases computation while enhancing understanding. For numerical validation purpose we solve a potential flow problem which satisfies Laplace equation, then we solve two-dimensional acoustics type problem which satisfies Helmholtz equation. Finally, we take a Poisson's equation problem as a case study, compare results with finite difference method and do some mesh convergence study.

Chapter 1

Introduction

1.1 Prelude

Acoustics engineering is an engineering branch which deals with the application of vibration and sound in technology. As we know sound pollution is a massive problem in today’s world. Severe problems of noise pollution include hearing loss, lack of concentration, headache etc. So, noise control is very much essential. One of the goal of acoustics engineering problem is the reduction of unwanted noise that is noise control. Besides noise control, acoustical engineering also tries to develop positive uses of sound in ultrasound medicine, designing auditoria etc. In civil structures noise suppression is an important problem. Acoustic engineering is a very important problem in the field of civil and mechanical engineering.

Engineering problems have complex domains and boundary conditions, which make them difficult to solve using analytical methods. Thus, to solve practical engineering problems sufficiently accurately (error is within permissible limit) we have to resort to some numerical technique. Generally, during solving numerical problems the entire body is divided into smaller segments and then, to adequately characterise the behaviour of the differential part of the body, several equations and relationships are used, finally further relationship developed to assemble these parts together. In most of the cases smaller parts is divided numeric solution become close to the actual solution but the operation time will increase.

There are mainly three approaches used for numeric solution (Ref. Fig. 1.3)

finite difference method (FDM), finite element method (FEM), boundary element method (BEM)

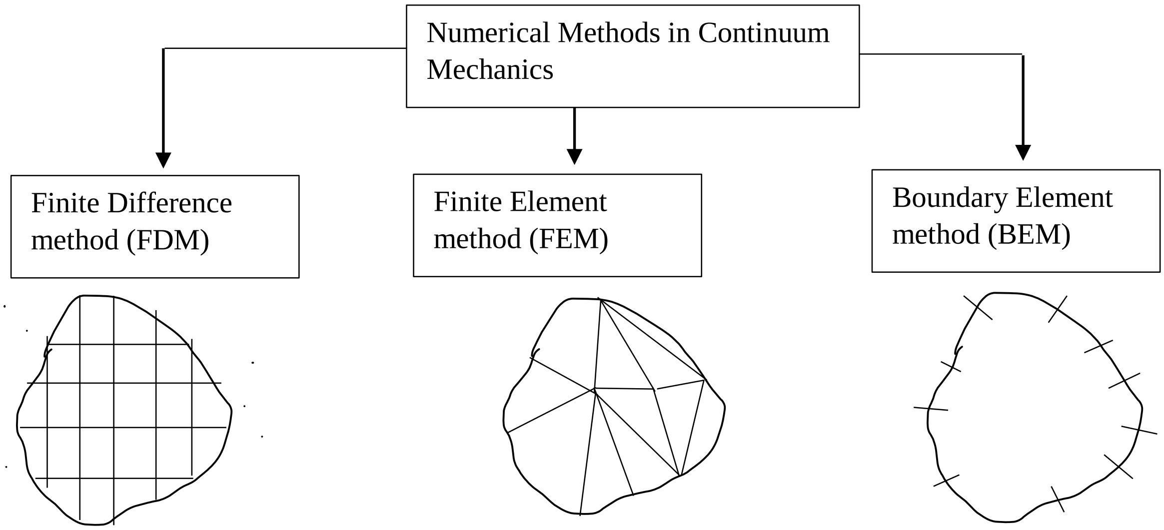

Internal Cells Domain Elements Boundary (Surface) Elements

Figure 1.1: Classification of numerical methods in continuum mechanics

FDM is the most straightforward of the three approaches. The governing partial differential equations are expressed as difference equations in this manner. As a result, inside the domain, a two-dimensional domain, grid, or cells is placed, and the difference approximation is applied to each of the inner points. As a result, a system of linear algebraic equations offers a unique solution if the actual problem's boundary conditions are met.

In the FEM technique, the solution domain is discretized into a small number of segments called elements. The governing differential equations define the behaviour of each element. All of these small components are assembled, and continuity and equilibrium requirements between adjacent portions are satisfied. A unique solution for entire linear algebraic equations can be found if the boundary conditions of the actual problems are met with a sparsely populated matrix. For practical engineering problems with complicated geometrics, the FEM is ideal.

BEM is a computer programme that analyses the behaviour of engineering structures and mechanical systems under external loads. BEM converts governing differential equations into integral identities that may be applied to a surface or a boundary. These integrals are numerically integrated over a boundary divided into discrete boundary segments known as boundary elements. Then a system of linear algebraic equations with boundary conditions appears, for which a unique solution can be found. However, for certain types of problems, FEM modelling can be unproductive and time-consuming.

1.2 Literature Review

About BEM

In early 1980’s the BEM was known as boundary integral equation method (BIEM). The base work of this work was done by **Green [1]** in 1828, When he used Green's function to solve Laplace type equations, he established the integral representation of the solution for the Dirichlet and Neumann problems.

In 1872 **Betti [2]** used a general method to integrate the elasticity equations and derivation of integral form solution. It is considered to be a straight forward development of Green’s theorem in Navier elasticity equations.

Betti's reciprocal theorem was utilised by **Somigliana [3]** in 1885 to derive an integral representation of solution for elasticity problem.

Singular boundary integral equations were initially used by **Fredholm [4]** to determine unknown boundary quantities and solve potential problems at the turn of the twentieth century. The boundary conditions for a well-posed mathematical physics problems were determined using this method as a mathematical tool but not as a solution method. This is logical because the analytical solution of the generated singular integral equations is not always attainable. The foundation of indirect BEM was laid by Fredholm integral equations.

Direct BEM is used when the unknown boundary quantities have a direct physical or geometrical meaning. Other BEM formulations in which the unknown boundary quantities do not have geometrical or direct physical meaning, such formulations fall into the class of indirect BEM.

Jawson [5] and **Symm [6]** discretized the integral equations of a two-dimensional potential problem represented as Laplace equation into straight line elements with constant potential functions. Except for some singular integrals that were integrated analytically, the elements are described in terms of nodal points, with integrations made using Simpson's rule. As the functions employed to formulate the problem are not imaginary and may be differentiated or integrated to determine physical values, their approach is referred to as **"semi-direct"**. They proposed a more generic formulation based on Green's third identity, with potentials and derivatives as the boundary unknown, and the results of this formulation were expressed **[5]** and **[7]**.

For solving of the Neumann-type boundary value problem, **Hess and Smith [8]** described the technique for developing a completely new method of solving general engineering problems. However, using the **indirect boundary element** technique, Hess and Smith constructed a number of strong programmes to obtain the Laplace type boundary value problem solution and applied it to potential flow and arbitrary bodies. To increase computer performance, the influence coefficients were analytically calculated in case of two- and three-dimensional instances, the equations were solved by iteration using the Gauss-Seidel method, and multipole expansions were used to determine elemental effect placed far away from the real node.

It's impossible to say who was the first to adopt the "direct" way of analysis. From an engineering standpoint, **Cruse and Rizzo's [9]** work in elastostatics is thought to have inspired the approach. For engineering and physical science problems, the direct method is the most appealing. Rizzo's work was fundamental since he was the first to see the strong resemblance between potential theory and classical elasticity theory and to devise a numerical method for solving the problem. He discretized the boundary using straight-line elements, with functions (displacements and tractions in this case) considered constant over each element. Except for singular integrals, Simpson's rule was applied.

In 1978 the BEM is observed connecting other numerical techniques example given finite differences and finite elements, notably through the work of Brebbia's work and collaborations**.**

The boundary integral equations (BIE) formulation methods can be divided into three categories as follows:

The indirect BEM: This method is based on the use of fictional density functions to formulate the problem. Despite the fact that these density functions have no physical relevance, we can derive the actual displacements and stresses by integrating them. As a result, this method is referred to as "indirect" because actual displacements and stresses are not used right once.

Semi-direct BEM: In this method, the functions used to formulate the problem are linked to stress functions, which have a little more physical significance than fictitious density functions. To compute displacements and stresses, these functions can be separated or integrated.

Direct BEM: In this method, real physical quantities such as displacements and tractions are employed to formulate the integral equations from the start. Using reciprocal work theorems, partial differential equations of elasticity derived from equilibrium equations, constitutive relationships, and relationship of strain and displacement are converted into integral equations that can be applied to the boundary. This strategy is simpler to comprehend because it involves real quantities rather than a hypothetical problem. As a result, this strategy will be employed.

The BEM's efficiency drew researchers in and encouraged them to continue developing the technology. A large number of literature papers on BEM for tackling a wide variety of engineering challenges were found in the late 1980s. The fundamental goal of new improvements in BEM is to overcome any method flaws that may arise. They attempt to tackle complex time-dependent problems, as well as linear and nonlinear problems for which the underlying solution is unknown. The resulting integral solution for all of these types of problems involves domain integrals, which makes the method more difficult to apply.

The dual reciprocity method (DRM) and the analogue equation method (AEM) are the most efficient techniques for successfully overcoming most of the obstacles such as domain integration while maintaining the BEM's purely boundary only feature.

About Dual Reciprocity Boundary Element Method (DRBEM)

DRM was first introduced by **Nardini and Brebbia [10]** in 1982 for solving elastodynamic problems. They actually intended to avoid the use of dynamic fundamental solution for solving the wave equation. **Wrobel *et al.* [11]** extended the concept to time-dependent diffusion problems in 1986. At 1990s **Partridge, Brebbia [12]** extends this method to solve general type of problems. DRBEM is a generic method for constructing particular solutions. DRBEM can be applied for huge number of partial differential equation and also time dependent problems without using their fundamental solutions. Two-dimensional Laplace equation, Poisson's, Helmholtz type equations, diffusion type equation and also three-dimensional problems are solved by DRBEM, discussed in **WT Ang [13]**. **Brebbia and Domingue [14]** in his book described solution of Potential problems (Laplace, Poisson's, Helmholtz equations), elastostatics problems using constant, linear and quadratic elements. **J.T. Katsikadelis [15]** in his book discuss about solving procedure for various types of equations by DRBEM. While DRBEM has been used to solve problems in interior **([10],[11],[12]** etc.), but lesser effort has been employed to solve exterior types of problems (where domain is unbounded) using DRBEM. Due to speciality of exterior problem, extension of interior problems to exterior problem is conceptually different. The approach of solving problems was first proposed by **Loeffler and Mansur [16]** in 1988 but as pointed out by **Zhu and Zhang [17]** in 1992 that the solution is not complete and satisfactory. They applied a new approach **([17],[18])** and applied to a number of practical engineering problems and got satisfactory results.

The convergence study of DRBEM is carried out by **Jumarhon, Amini, and Chen [19]** for solving Poisson's equation with Dirichlet boundary condition by applying radial basis function approximation.

Marin *et al.* [20] used the dual reciprocity boundary element approach to solve the Cauchy type problem for Helmholtz type equations with variable coefficients. The suggested numerical method's accuracy, convergence, and stability with regard to various approximation functions, DRBEM discretization, and various amounts of noise inserted in the boundary data are also examined.

Development of Acoustics Engineering

Study of science of sound or acoustics is from the ancient times. Ancient Greeks and Chinese philosophers tried to study the nature of sound. As an old philosopher, Leonardo da Vinci (1452–1519) stated that there can be no sound if there is no movement of the air. His findings led him to believe that the waves formed by a stone thrown into water were similar to the transmission of sound waves. These studies and research did not result in significant advancements in acoustics until the seventeenth century, when a link between pitch and frequency was discovered. **Marin Mersenne [21]** demonstrated the absolute frequency ratio of two vibrating strings, radiating a musical note and its octave, then frequency ratio 1:2. The air motion caused by musical sounds was considered to be oscillatory in nature, and it was discovered that sound travels at a finite speed. Mersenne was called father of modern acoustics. Independently of Mersenne, **Galileo Galilei [22]** discussed on frequency equivalence. **Joseph**

Sauveur first mentioned the term *acoustics* for the science of sound. Hooke developed the basis of vibration and elasticity theories in 1678 when he derived the law connecting force to deformation. **Ernst F.F. Chladni [23]** established the field of modern experimental acoustics through discovering torsional vibrations and velocity measurements with the help of vibrating rod and resonating pipe. **Newton [24]** derived theoretically the speed of sound.
Sabine [25] developed at an empirical relevance among room's reverberation qualities, its size as well as the amount of absorbent material. He relates reverberation time (T) of a room, its volume (V) and total sound absorption or absorption area (A) in the form $T \propto \frac{V}{A}$

Numerical Solution of Acoustic Problems

Kirkup and Amini [26] considered the numerical solution of the Helmholtz eigen value problem. Two-dimensional acoustics equation satisfies Helmholtz type equation. When the boundary element approach is used, it converts the problem to a non-linear eigen value problem. The nonlinear eigenvalue problem is transformed into a typical generalised boundary value problem. This method is used to solve a two-dimensional sphere and a three-dimensional sphere test problem with axisymmetric boundary conditions.

Kirkup and Jones [27] considered computational technique for acoustics modal analysis of an enclosed fluid. The finite element method is discussed in this study, as well as the boundary integral equations method. The physical significance of a loudspeaker's interior acoustic resistances is examined. This paper investigates the practical application of the boundary element method to the interior acoustic modal analysis problem. The dual reciprocity and multiple reciprocity methods are thoroughly described.

In **Kirkup and Amini [28]** Green's formula-based boundary integral equations for the Helmholtz problem for exterior domain are considered. The boundary integral equations may be Fredholm first kind, second kind, or hyper-singular type, and collocation methods are employed to discretize them. The impact of quadrature error on the precision of discrete collocation methods is comprehensively investigated.

Kirkup [29] described Boundary element method and investigated with respect to its application to exterior two-dimensional Laplace type equations. Analyses are carried out using both empirical and algebraic methods. The boundary element approach is discussed for solving Helmholtz problems with generic boundary conditions. For acoustical radiation problems, boundary element approaches and Rayleigh integral methods are presented and illustrated.

Kirkup [30] used of the boundary element method to solve acoustics or Helmholtz type problems. First, the BEM foundation is established for Laplace's equation. For both interior and exterior acoustic problems, the boundary integral is specified, and BEM is determined using collocation. The current state of research in coupling the boundary element approach to other methods for solving vibro-acoustic, aero-acoustic, and inverse problems via BEM is reviewed. There are references to BEM applications in each area of acoustics. Problem complexity and solutions for reducing complexity are discussed.

Kirkup [31] discussed the boundary element technique in acoustics in depth in his book. In Helmholtz form, the wave equation was created and numerically solved using Fortran programming. The boundary or surface is represented by a set of panels, each having a simple parametric form for the boundary functions, and the boundary integral problem is reduced to a linear system of equations, allowing for a numerical solution. The integral equation is simplified to discrete form, and the acoustic problems are solved using two-dimensional boundary, three-dimensional surface, and axisymmetric surface meshes.

Raichel [32] discuss on the acoustics science and its application. It is a good book to study acoustics.

Kinsler *et al.* [33] in his book discuss fundamental theories of acoustics. This is also a very good book to understand the basic of acoustics.

Baby, Mathew *et al.* [34] discuss on the feasibility study of civil engineering buildings and acoustics problems related to it. It discusses the effects of important parameters that the buildings can be influenced.

Drozdek, Majchrzak [35] used DRBEM for solution of bio-heat transfer through skin surface that is governed by **Pennes** bio-heat equation **[36]**

$x \in \Omega: \lambda \nabla^2 T(x) + c_B G_B [T_B - T(x)] + Q_{met} = 0$

where $\lambda [W/mK]$ is the thermal conductivity, $Q_{met} W/m^3$ is the metabolic heat source, G_B $[m^3/s/m^3$ tissue] is the blood perfusion rate, $c_B [J/m^3 K]$ is the volumetric specific heat of blood, T_B is the arterial blood temperature, T denotes the temperature, $x = \{x_1, x_2\}$.

Generalized inhomogeneous Helmholtz equation with variable coefficients is valid in cases of seismology, wave mechanics, anisotropic mechanics of materials, acoustics and so on. **Gumerov and Duraiswami [37]** has shown how the Helmholtz equation can also be derived from the heat conduction equation, the Schrodinger equation, the telegraph equations, and for the case of acoustics. From a mathematical point of view, it could also be visualized as an eigenvalue problem for the Laplace operator.

1.3 Advantages and Disadvantages of BE

Any problem's dimensionality is reduced by one while solving it by BEM. We may use a three-dimensional cuboidal domain for explanation. To analyze by FEM let's induce 9 cuts each along X, Y and Z directions, resulting in 10*10*10 =1000 three dimensional elements.

In contrast, for the same degree of accuracy, BEM will require only 10*10*6 = 600 two-dimensional surface elements.

For mesh convergence study, if we intend to have 20 elements per direction, number of finite elements become 20*20*20 = 8000 solid elements, whereas the BE analysis will employ 20*20*6=2400 surface elements.

Thus, from the above discussion, it is clear that computation time and computational storage space required for BEM is lesser than the other two methods. Hence, BEM has been preferred over FDM and FEM for this study.

Thus, **the merits of BEM** are as follows:

1. Less data preparation time: This is a direct result of the 'surface only' modelling, which shrinks the problem by one dimension. Due to this, the amount of time needed to prepare data is considerably decreased.
2. High resolution of stresses: Because no further approximation is made to the solution at the interior locations, the stresses are precise (and totally continuous) inside the domain. As a result, the BE method is well suited for modelling quickly changing stresses including fracture, contact problems, and stress concentration.

3. Less computer time and storage: To achieve the same level of accuracy, the BE approach uses fewer nodes and elements but a fully populated matrix. In BE solutions, the level of approximation is limited to the surface.
4. Less unwanted information: While modelling a three-dimensional complex body by FEM, one calculates stress at all nodal points, which is inefficient since such stress values are required at only a few locations while designing. In BEM internal points are interactively obtained at some particular interior region as per designer's choice rather than the entire region.
5. It's simple to use for incompressible materials.

Few Disadvantages of BEM

1. Unfamiliar mathematics: The mathematics involved in BEM is not quite easy and needs some knowledge of advanced mathematics to learn.
2. Necessity of the fundamental solution to the governing equation: BEM make use of an idea like Betti's reciprocal theorem where a fully known solution and a partly known solution is coupled and solved. The fundamental solution, alias, Green's function is used to define the known solution, and thus essential to know before we attempt the solution by BEM. Certain fundamental solutions are unknown, some are difficult to handle.
3. Fully populated solution matrix: Unsymmetrical solution matrix, fully populated with generally non-zero coefficients.
4. In non-linear problems like elasto-plasticity, the interior must be modelled in full without reduction of dimensionality. However, the method is still very accurate.

1.4 Objective

From the literature reviews it has been understood that in various engineering problems, the Helmholtz equation needs to be solved in different forms. Hence, the concept of a generalized Helmholtz equation with variable coefficients appeared.

Further, the efficiency of BEM over FDM or FEM, regarding the computation time, data preparation and data churning, is also clear. Vis-à-vis, we require fundamental solution, or, Green's function, for each of such equations before we solve the same using the conventional BEM, which is not very alluring. The Dual Reciprocity BEM, on the other hand, make use of the fundamental solution for the simpler Laplace equation, to bypass this problem in a easier manner.

Thus, the **objective** of the present research is to make an attempt is made to master the boundary element technique and implement this to solve a range of practical engineering problems, by solving the generalized Helmholtz equation with variable coefficients.

However, the **scope** of the present research is delimited to

- Two-dimensional domains, for better visualization
- Use of constant elements, for easier computing, and
- Study of specifically acoustics problem only,
- Initially the Laplace equation is explored for the understanding of the conventional boundary element method, and then

- We go for solution of the generalized Helmholtz equation with variable coefficients using dual reciprocity boundary element method.

Now we move on to develop the conventional boundary element formulation for Laplace type equations using constant elements and we will validate the numerical results.

Chapter 2

Boundary Element Analysis of Laplace Equation

2.1 Introduction

From the discussion in previous chapter, it is clear that the two-dimensional Laplace equation is the easiest avenue to delve with boundary element formulation. Understanding this formulation is necessary when we try to go forward to solve other complex type problems using boundary element method. Hence, we will take the help of various references [11, 12,13, 14, and 15] to understand the direct formulation. We first we broadly outline the boundary element treatment of two-dimensional Laplace equation. Next the formulae for constant boundary elements are derived. Then to numerically validate the program developed, we solve a potential problem which satisfies Laplace equation.

So, we begin our study of boundary element methods by attempting to solve a boundary value problem governed by the two-dimensional Laplace equation, which is given by

$$\frac{\partial^2\varphi}{\partial x^2} + \frac{\partial^2\varphi}{\partial y^2} = 0 \qquad (2.1)$$

The boundary value problem in the two-dimensional region R (in figure 2.1 on the OXY plane) is confined by closed curve C which has boundary conditions as given below

A) "Essential" boundary condition

$$\varphi = f_1(x,y) \quad \text{for } (x,y) \in C_1 \qquad (2.2a)$$

B) "Natural" boundary condition

$$\frac{\partial\varphi}{\partial n} = f_2(x,y) \quad \text{for } (x,y) \in C_2 \qquad (2.2b)$$

C_1, C_2 are non-intersecting curves while f_1 and f_2 are known functions. So, $C_1 \cup C_2 = C$

(Refer: figure 2.1)

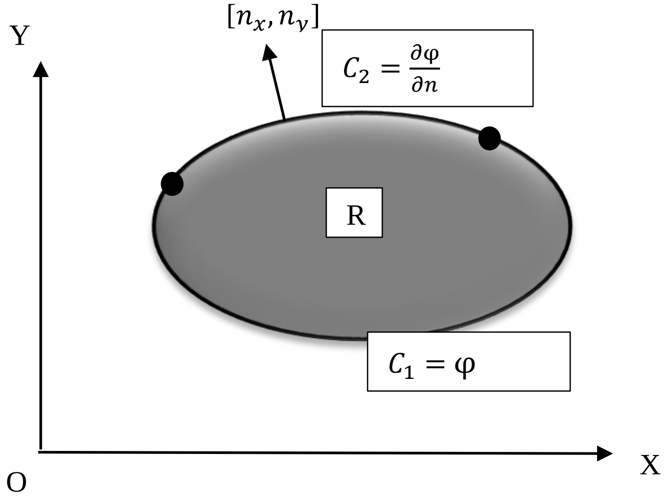

Figure 2.1: Domain R with mixed boundary conditions

Normal derivative ($\frac{\partial \varphi}{\partial n}$) as per equation (2.2) can be defined as

$$\frac{\partial \varphi}{\partial n} = n_x \frac{\partial \varphi}{\partial x} + n_y \frac{\partial \varphi}{\partial y} \tag{2.3}$$

(n_x, n_y) are called unit normal vector of X and Y components to the curve C. $[n_x, n_y]$ are pointing away from C and can be changed from one point to other point on curve C.

$[n_x, n_y]$ is the function of x and y.

If the boundary conditions in equation (2.2) are properly defined, then the boundary value problem gives only one and unique solution at any given location of the boundary. At each node either we know the potential or flux.

In general, getting an accurate solution from equations (2.1) and (2.2) is challenging. Because of the complex geometrical nature of the region and boundary conditions, there are some mathematical complications in actual engineering challenges.

2.2 Fundamental solution

Now, we consider a unit point load source acting at a point $P(\xi, \eta)$ of the $xy -$ plane. At the point $P(\xi, \eta)$ density due to point load is infinite as if we apply a point load at that point area tends to zero. Density at any arbitrary point $Q(x, y)$ can be mathematically written by using delta function as below

$$f(Q) = \delta\,(Q - P) \tag{2.4}$$

and the equation is satisfied by the potential $\varphi_1 = \varphi_1(Q, P)$ created at point Q

$$\nabla^2 \varphi_1 = \delta\,(Q - P) \tag{2.5}$$

The 'fundamental solution' of the potential is the particular solution of equation (2.5). The 'fundamental solution' φ_1 denotes the field which is produced by a concentrated unit point source located at the point P. The source's effect is transmitted from P to infinity without any regard for boundary conditions. Dirac delta function has the property of going to infinity at the source point P and zero elsewhere. Dirac delta function's integral over the domain is equal to unity.

If we use polar coordinates (r, θ) whose center is (0,0), we can rewrite equation (2.1) in the form of polar coordinate equation (refer APPENDIX-A, Section A.1, equation A.3) as

$$\frac{1}{r}\frac{\partial}{\partial r}\left(r \frac{\partial \psi}{\partial r}\right) + \frac{1}{r^2}\frac{\partial^2 \psi}{\partial \theta^2} = 0 \tag{2.6}$$

When ψ is not dependent on θ that means ψ is only function of r. Then we can write equation (2.6) as

$$\frac{d}{dr}(r \frac{d}{dr}[\psi(r)] = 0 \; for \; r \neq 0 \tag{2.7}$$

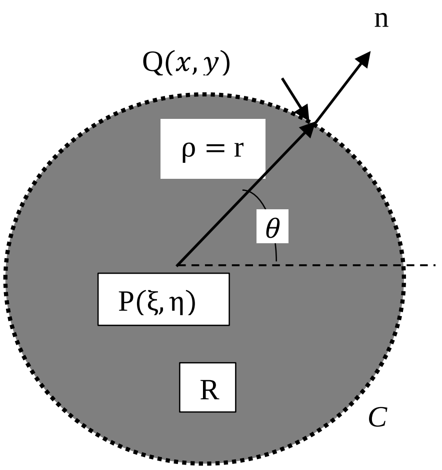

Figure 2.2: Circular domain R with radius ρ a point source P in it's centre.

If this ordinary differential equation is integrated twice, we can get the following equation

$$\psi(r) = A\, ln(r) + B \tag{2.8}$$

where A and B are arbitrary constants.

We can set $B = 0$ because we are seeking for a specific solution.

We assume circular domain R with radius ρ whose centre is P (Refer: Figure 2.2). As the problem is axisymmetric with respect to source

$$\frac{d\psi}{dn} = \frac{d\psi}{dr} = A\frac{1}{r} \quad \text{and} \quad ds = r\, d\theta \tag{2.9}$$

Let us apply Green's identity as per equation (A.20) (reference Appendix A, section A.4) for $u = 1$ and $v = A \ln r$, yields

$$\int_{\mathrm{R}} \nabla^2 u\, dR = -\int_{\mathrm{C}} \frac{dv}{dn}\, ds$$

Using equation (2.5) and equation (2.9) the relation the boundary C and radius ρ centred at P.

$$-\int_R \delta\,(Q - P)\, dR = -\int_0^{2\pi} A\frac{1}{\rho}\, \rho\, d\theta$$

Or, $1 = 2\pi A$

Or, $A = \frac{1}{2\pi}$ (2.10)

Hence, the fundamental solution becomes,

$$\psi(r) = \frac{1}{2\pi} ln(r) \tag{2.11}$$

$\psi(r)$ is the fundamental solution in terms of polar coordinates. We will convert it in cartesian coordinate $\varphi_1(x, y)$ is fundamental solution in cartesian coordinate.

$$\varphi_1(x, y) = \frac{1}{2\pi} ln(\sqrt{x^2 + y^2}) \quad for\ (x, y) \neq 0 \tag{2.12}$$

Now, if we move polar coordinate centre from (0,0) to a general point (ξ, η) then particular solution become

$$\varphi_1(x, y) = \frac{1}{2\pi} ln(\sqrt{(x - \xi)^2 + (y - \eta)^2}\,)\ for\ (x, y) \neq (\xi, \eta) \tag{2.13}$$

If we specifically use the symbol $\Phi\ (x, y; \xi, \eta)$, to designate particular solution then it can be written

$$\Phi\ (x, y; \xi, \eta) = \frac{1}{4\pi} ln((x-\xi)^2 + (y-\eta)^2) \qquad (2.14)$$

This fundamental solution value does not change, if we interchange the points P and Q.

$\varphi_1(P, Q) = \varphi_1(Q, P)$

2.3 Direct BEM for the Laplace equation

The solution to the Laplace equation will be developed here as given in equation (2.1) and must satisfy equations (2.2) boundary conditions.

Then if we apply Green's identity equation (A.20) for the functions φ_1, φ_2 satisfies equation (2.5) and equation (2.1) respectively and assuming source point as P.

$$-\int_R \varphi(Q)\, \delta\, (Q - P)\, dR = \int_C \left(\varphi_1(q, P)\frac{\partial\varphi_2(q)}{\partial n_q} - \varphi_2(q)\frac{\partial\varphi_1(q,P)}{\partial n_q}\right) ds_q \qquad (2.15)$$

Where $P, Q \in R$ and $q \in C$

Points inside domain (R) are denoted in capital letters, like, P, Q and points on the boundary are defined by lowercase letters p, q.

Applying the property of Dirac Delta function (Refer section A.5, equation A.26) in equation (2.15) we can write,

$$\varphi(P) = -\int_C \left(\varphi_1(q, P)\frac{\partial\varphi_2(q)}{\partial n_q} - \varphi_2(q)\frac{\partial\varphi_1(q,P)}{\partial n_q}\right) ds_q \qquad (2.16)$$

where φ_1 and $\frac{\partial\varphi_1}{\partial n}$ are both known quantities. These represent the fundamental solution of the Laplace equation and flux at point q of the boundary. Given in the following equations.

$$\varphi_1 = \frac{1}{2\pi} ln(r) \qquad (2.17)$$

$$\frac{\partial\varphi_1}{\partial n} = \frac{1}{2\pi}\frac{\cos\theta}{r} \qquad (2.18)$$

Refer equation (A.38) Appendix-A, Section A.6

We can write, $\varphi_1 = \Phi\ (x, y; \xi, \eta)$ and $\varphi_2 = \varphi$

The differential equation's solution (2.1) at any point P which is inside the domain can be represented in terms of boundary values of φ and its normal derivative $\frac{\partial\varphi}{\partial n}$. Equation (2.16) can be termed as *integral representation of the solution* for Laplace equation. Either φ or $\frac{\partial\varphi}{\partial n}$ will be defined at any point on the boundary (say $q(x, y)$). To determine the solution from the integral representation that is given in equation (2.16) where either φ or $\frac{\partial\varphi}{\partial n}$ is not prescribed, may be obtained by calculating the integral representation of φ for points $P \equiv p$ on boundary C.

We look at the general example of non-smooth boundary and P is the corner point in figure 2.3. Consider the domain R^* resulting from R after deleting a small section P is the center, which has radius of ϵ and is bounded by the arcs PA and PB. The sum of arcs AP and PB is denoted by l while C_ϵ denotes circular arc AB. The outward normal of C_ϵ coincides with radius ϵ and directed towards centre P. At point P the angle between tangents of the boundary is indicated by α.

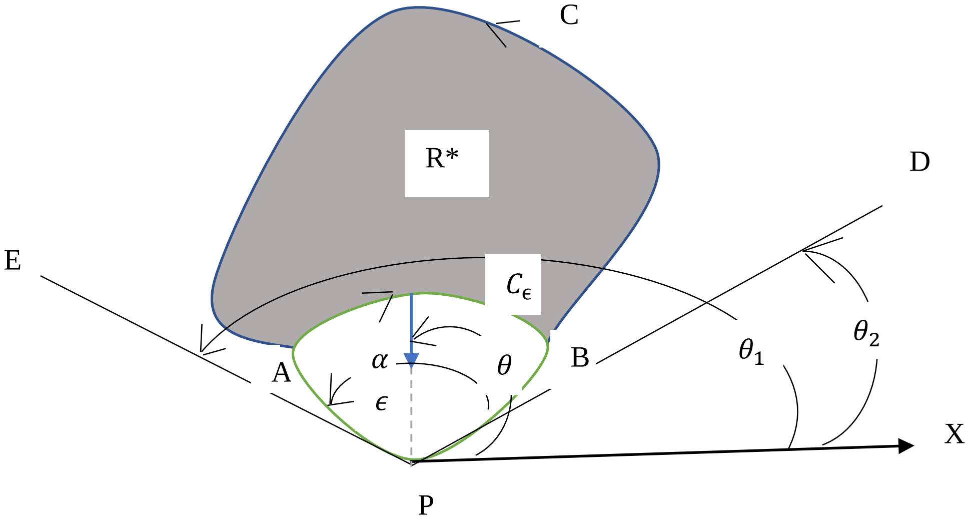

Figure 2.3: Geometric definitions for a non-smooth boundary's corner point P.

$$\lim_{\epsilon\to 0}(\theta_1-\theta_2)=\alpha$$
$$\lim_{\epsilon\to 0}(C_\epsilon)=0$$
$$\lim_{\epsilon\to 0}(C-\mathrm{l})=C$$

Now, apply Green's identity equation (Ref. equation A.20) in R^* domain for the function φ_1, φ_2 satisfying equations (2.1) and (2.5). As P point lies outside the domain R^*, where $\delta\,(Q-\;P)=0$, so

$$\int_R \varphi\delta\,(Q-\;P)\,dR=0$$

As a result, Green's identity gives,

$$0=\int_{C-l}\left(\varphi_1\frac{\partial\varphi_2}{\partial n_q}-\varphi_2\frac{\partial\varphi_1}{\partial n_q}\right)ds+\int_{C_\epsilon}\left(\varphi_1\frac{\partial\varphi_2}{\partial n_q}-\varphi_2\frac{\partial\varphi_1}{\partial n_q}\right)ds \qquad (2.19)$$

Now we will see the case when $\epsilon\to 0$ the first part of the integral will become

$$\lim_{\epsilon\to 0}\int_{C-l}\left(\varphi_1\frac{\partial\varphi_2}{\partial n_q}-\varphi_2\frac{\partial\varphi_1}{\partial n_q}\right)ds=\int_C\left(\varphi_1\frac{\partial\varphi_2}{\partial n_q}-\varphi_2\frac{\partial\varphi_1}{\partial n_q}\right)ds \qquad (2.20)$$

Second part of equation can be written as

$$\int_{C_\epsilon}\left(\varphi_1\frac{\partial\varphi_2}{\partial n_q}-\varphi_2\frac{\partial\varphi_1}{\partial n_q}\right)ds=\int_{C_\epsilon}\frac{1}{2\pi}\frac{\partial\varphi}{\partial n}\ln r\;ds-\int_{C_\epsilon}\frac{1}{2\pi}\,\varphi\frac{\cos\theta}{r}\;ds=\;I_1+I_2 \qquad (2.21)$$

For circular arc C_ϵ $r = \epsilon$ and $\theta = \pi$. Moreover, $ds = \epsilon(-\,d\theta)$. As θ is positive in anti-clockwise which is opposite direction of s. So, first integral we can write

$$I_1 = \int_{C_\epsilon} \frac{1}{2\pi}\frac{\partial\varphi}{\partial n} ln\, r\ \ ds = \int_{\theta_1}^{\theta_2} \frac{1}{2\pi}\frac{\partial\varphi}{\partial n}\epsilon\, ln\,\epsilon\ \ (-\,d\theta) \qquad (2.22)$$

The value of an integral is equal to the value of its integrand at some point O inside the integration interval multiplied by the length of that interval, according to the mean value theorem of integral calculus. Hence,

$$I_1 = \frac{1}{2\pi}(\frac{\partial\varphi}{\partial n})_o\, \epsilon\, ln\,\epsilon\ \ (\theta_1 - \theta_2)$$

As, $\epsilon \to 0$, the arc's O point approaches P point. At that case, $\frac{\partial\varphi}{\partial n}$ at P is confined though it is not defined. Moreover, it can be written as,

$$\lim_{\epsilon\to 0}(\epsilon \ln \epsilon) = 0$$

which implies

$$\lim_{\epsilon\to 0} I_1 = 0 \qquad (2.23)$$

Second part of the integral from equation (2.21) can be written as

$$I_2 = -\int_{C_\epsilon} \frac{1}{2\pi}\ \varphi\frac{\cos\theta}{r}\ ds = \ -\int_{\theta_1}^{\theta_2} \frac{1}{2\pi}\varphi\frac{-1}{\epsilon}\epsilon\ (-\,d\theta)$$

Or by applying the mean value theorem,

$$I_2 = -\frac{1}{2\pi}\varphi_o(\theta_2 - \theta_1) = \frac{(\theta_1-\theta_2)}{2\pi}\varphi_o$$

Finally,

$$\lim_{\epsilon\to 0} I_2 = \frac{\alpha}{2\pi}\ \varphi(p)\ ,\ p \equiv P \in C \qquad (2.24)$$

From equations (2.23), (2.24), (2.20) we get

$$\lim_{\epsilon\to 0}\int_{C_\epsilon}\left(\varphi_1\frac{\partial\varphi_2}{\partial n_q} - \varphi_2\frac{\partial\varphi_1}{\partial n_q}\right)ds = \frac{\alpha}{2\pi}\ \varphi(p) \qquad (2.25)$$

We can incorporate our findings from equations (2.20) and (2.25) and put into (2.19) for $\epsilon \to 0$

$$\frac{\alpha}{2\pi}\ \varphi(p) = -\int_{\mathrm{C}}\ \left(\varphi_1(q,P)\frac{\partial\varphi_2(q)}{\partial n_q} - \varphi_2(q)\frac{\partial\varphi_1(q,P)}{\partial n_q}\right)ds_q \qquad (2.26)$$

The integral representation of the Laplace equation's solution (2.1) is represented by equation (2.26) at the points $P \in C$, non-smooth boundary. In case of smooth boundary at those points p, $\alpha = \pi$. So, the equation (2.26) becomes

$$1/2\ \ \varphi(p) = -\int_C\ \left(\varphi_1(q,P)\frac{\partial\varphi_2(q)}{\partial n_q} - \varphi_2(q)\frac{\partial\varphi_1(q,P)}{\partial n_q}\right)ds_q \qquad (2.27)$$

Now we compare equations (2.16) and (2.26) we can see that function φ is discontinuous when $P \in R$ is on the boundary. It shows a jump equal to $(1 - \frac{\alpha}{2\pi})\ \varphi(p)$ for corner points equation (2.26) or for smooth parts on the boundary $\frac{1}{2}\ \varphi(p)$ from equation (2.27). Now, we will see when the point P is outside the domain R. Again, apply Green's identity (ref. equation A.20)

$$0 = -\int_C\ \left(\varphi_1(q,P)\frac{\partial\varphi_2(q)}{\partial n_q} - \varphi_2(q)\frac{\partial\varphi_1(q,P)}{\partial n_q}\right)ds_q \qquad (2,28)$$

Now, we can write equations (2.16), (2.27) and (2.28) in combined form

$$\lambda(P)\ \varphi(P) = -\int_C\ \left(\varphi_1(q,P)\frac{\partial\varphi_2(q)}{\partial n_q} - \varphi_2(q)\frac{\partial\varphi_1(q,P)}{\partial n_q}\right)ds_q \qquad (2.29)$$

From this expression if coordinate of P is (ξ, η) and coordinate of q is (x, y). The $\varphi_1(q, P)$ or $\Phi(x, y; \xi, \eta)$ is the fundamental solution defined in equation (2.14)

The we can rewrite equation (2.29) changing sign in right hand side as

$$\lambda(\xi, \eta)\, \varphi(\xi, \eta) = \int_C \left(\varphi(x, y) \frac{\partial \Phi(x,y;\xi,\eta)}{\partial n} - \Phi(x, y; \xi, \eta) \frac{\partial \varphi(x,y)}{\partial n}\right) ds(x, y) \qquad (2.30)$$

$\lambda(\xi, \eta)$ is called as free term coefficient, depends on the location of point (ξ, η) and defined as below

$\lambda(\xi, \eta) = 1$ for P inside R

$= \frac{1}{2}$ for $P \equiv p$ on the boundary C

$= 0$ for P outside R

2.4 Boundary element solution using constant element

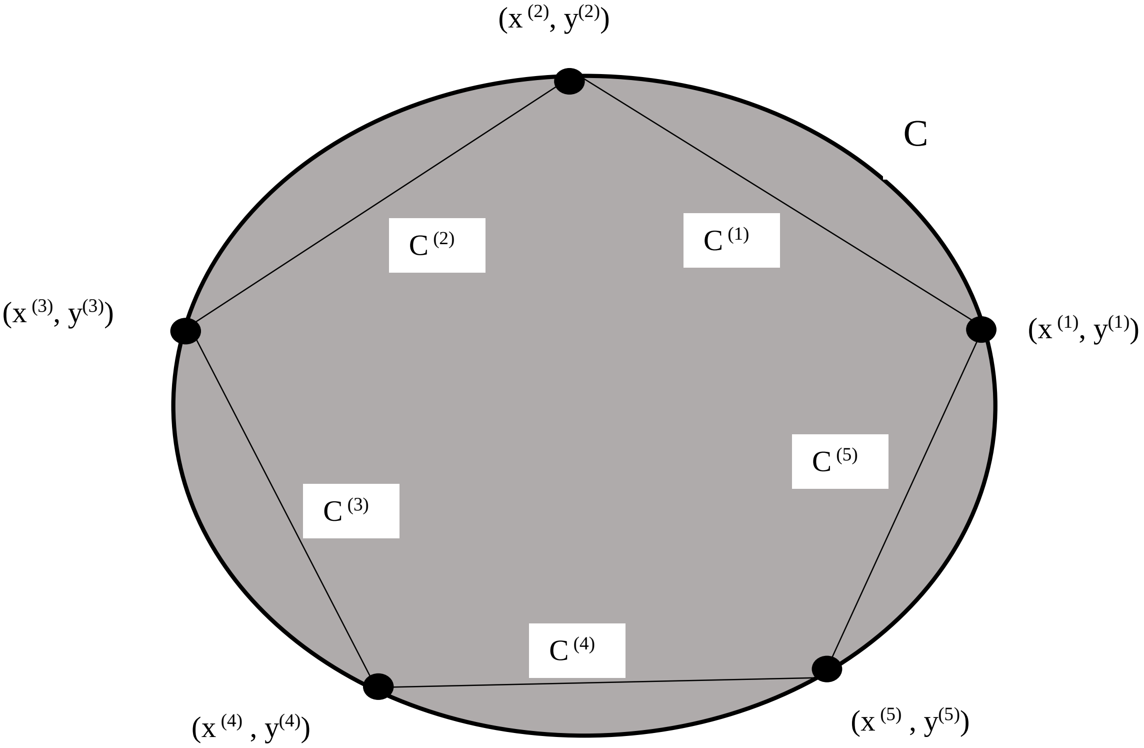

Figure 2.4: Constant elements representation

Now we will use equation (2.29) in a simple boundary element technique to solve an interior boundary value problem which is defined as equation (2.1) and (2.2).

The boundary portion C is divided approximately as N-sized polygon whose sides or boundary elements are defined as $C^{(1)}, C^{(2)}, \ldots, C^{(N-1)}, C^{(N)}$.

$$C \cong C^{(1)} \cup C^{(2)} \cup \ldots\ldots \cup C^{(N-1)} \cup C^{(N)} \qquad (2.31)$$

Now, in the anti-clockwise direction we place N well-spaced points $(x^{(1)}, y^{(1)})$, $(x^{(2)}, y^{(2)})$..., $(x^{(N-1)}, y^{(N-1)})$, $(x^{(N)}, y^{(N)})$ on C. We can define $(x^{(N+1)}, y^{(N+1)}) = (x^{(1)}, y^{(1)})$ and we

consider $C^{(k)}$ to be the boundary element between $(x^{(k)}, y^{(k)})$ to $(x^{(k+1)}, y^{(k+1)})\ for\ k = 1, 2, \dots, N$.
Figure (2.4) shows how the boundary is approximated by five boundary elements named $C^{(1)}, C^{(2)}, C^{(3)}, C^{(4)}\ and\ C^{(5)}$.
For a simpler case is assumed constant boundary element functions φ and $\frac{\partial\varphi}{\partial n}$ on the boundary C. Our approximation can be written in this way

$$\varphi \cong \varphi^k\ and\ \frac{\partial\varphi}{\partial n} = p^k \text{ for } (x, y) \in C^{(k)}\ (for\ k = 1,2, \dots, N), \tag{2.32}$$

where φ^k and p^k are the values of φ and $\frac{\partial\varphi}{\partial n}$ at the midpoint of the element $C^{(k)}$

From equations (2.31) and (2.32) the equation (2.30) can be written as F

$$\lambda(\xi,\eta)\varphi(\xi,\eta) = \sum_{k=1}^{N}\{\varphi^k F_2^k(\xi,\eta) - p^k F_1^k(\xi,\eta)\} \tag{2.33}$$

where

$$F_1^k(\xi,\eta) = \int_{C^{(k)}} \Phi(x, y; \xi, \eta)\, ds(x, y)$$

$$F_2^k(\xi,\eta) = \int_{C^{(k)}} \frac{\partial}{\partial n}[\Phi(x, y; \xi, \eta)]\, ds(x, y) \tag{2.34}$$

For a given k value, either φ^k(potential) or p^k (flux) is known from boundary conditions that is given in equation (2.2). So, there are N unknowns on the right-hand side of equation (2.33). To evaluate the unknowns, we have N number of equations.
Let, (ξ, η) in equation (2.33) be the midpoints of $C^{(1)}, C^{(2)}, \dots, C^{(N-1)}, C^{(N)}$ then we obtain,

$$\frac{1}{2}\varphi^m = \sum_{k=1}^{N}\{\varphi^k F_2^k(x^m, y^m) - p^k F_1^k(x^m, y^m)\}$$

$$For\ m = 1,2, \dots\dots, N, \tag{2.35}$$

Where (x^m, y^m) is the midpoint of $C^{(m)}$
In equation (2.35), $\lambda(x^m, y^m) = \frac{1}{2}$,
(x^m, y^m) is the midpoint of $C^{(m)}$and is located the smoother portion of the approximate boundary $C^{(1)} \cup C^{(2)} \cup \dots\dots \cup C^{(N-1)} \cup C^{(N)}$
Equation (2.35) constitutes N linear equations with N unknowns on the right-hand side of equation (2.33). We can write with proper arrangement

$$\sum_{k=1}^{N} a^{(mk)} z^{(k)} = \sum_{k=1}^{N} b^{(mk)} \quad for\ m = 1,2, \dots\dots, N \tag{2.36}$$

Where $a^{(mk)}$, $b^{(mk)}$ and $z^{(k)}$ are defined by,

$$a^{(mk)} = -F_1^k(x^m, y^m) \qquad \text{when } \varphi \text{ is specified over } C^{(k)}$$

$$= F_2^k(x^m, y^m) - \frac{1}{2}\delta^{(mk)} \qquad \text{when } \frac{\partial\varphi}{\partial n} \text{ is specified over } C^{(k)}$$

$$b^{(mk)} = \varphi^k(-F_2^k(x^m, y^m) + \frac{1}{2}\delta^{(mk)} \qquad \text{when } \varphi \text{ is specified over } C^{(k)}$$

$$= p^k F_1^k(x^m, y^m) \qquad \text{when } \frac{\partial\varphi}{\partial n} \text{ is specified over } C^{(k)}$$

$$\delta^{(mk)} = 0 \quad \text{if } m \neq k$$

$$= 1 \quad \text{if } m = k$$

$$z^{(k)} = p^k \qquad \text{when } \varphi \text{ is specified over } C^{(k)}$$

$$= \varphi^k \qquad \text{when } \frac{\partial\varphi}{\partial n} \text{ is specified over } C^{(k)}$$

(2.37)

$z^{(1)}, z^{(2)}, \dots\dots, z^{(N-1)} z^{(N)}$ are N number of unknown constants of right-hand side of equation (2.33) and $a^{(mk)}, b^{(mk)}$ are known coefficients.

When we can get the unknown values of $z^{(1)}, z^{(2)}, \ldots\ldots, z^{(N-1)}, z^{(N)}$ the values of $\varphi, \frac{\partial\varphi}{\partial n}$ over $C^{(k)}$ element that is φ^k, p^k are known for $k = 1,2,\ldots.,N$ then the equation (2.33) with $\lambda(\xi,\eta) = 1$ gives an explicit formula for calculation of φ in interior of R, that is,

$$\varphi(\xi,\eta) = \sum_{k=1}^{N}\{\varphi^k F_2^k(\xi,\eta) - p^k F_1^k(\xi,\eta)\} \quad \text{for } (\xi,\eta) \in R \tag{2.38}$$

Formulas for calculating $F_1^k(\xi,\eta)$ and $F_2^k(\xi,\eta)$ as per equation (2.33) is given below section.

2.5 Formulae for integrals of constant elements

The functions $F_1^k(\xi,\eta)$ and $F_2^k(\xi,\eta)$ are defined in terms of line integral over $C^{(k)}$ as per equation (2.34). Now analytically, we will solve this.

By using parametric equation, we can describe the points on element $C^{(k)}$ as

$$x = \mathrm{x}^{(k)} - tl^{(k)}{n_y}^{(k)}$$
$$y = y^{(k)} + tl^{(k)}{n_x}^{(k)} \tag{2.39}$$

Where 't' varies from 0 to 1

Where $l^{(k)}$ is the length of $C^{(k)}$ and $[{n_x}^{(k)}, {n_y}^{(k)}] = [y^{(k+1)} - y^{(k)},\ x^{(k)} - x^{(k+1)}]\ /\ l^{(k)}$ (refer figure 2.5) is the unit normal vector to $C^{(k)}$ pointing away from R.

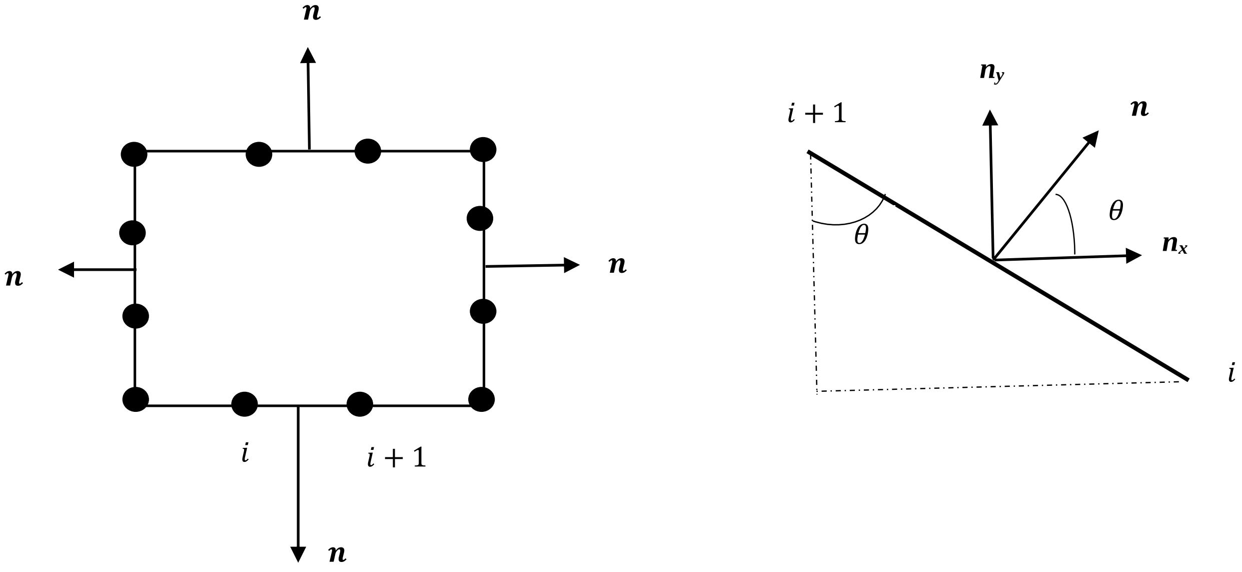

Figure 2.5: Formula development for constant element

for $(x,y) \in C^{(k)}$, we can write that $ds = \sqrt{(dx)^2 + (dy)^2} = l^{(k)}\, dt$ and

$$(x-\xi)^2 + (y-\eta)^2 = A^{(k)}t^2 + B^{(k)}(\xi,\eta)t + E^{(k)}(\xi,\eta) \tag{2.40}$$

Let us replace x and y from equation (2.39), so that

$$\text{LHS} = \left(x^{(k)} - tl^{(k)}{n_y}^{(k)} - \xi\right)^2 + (y^{(k)} + tl^{(k)}{n_x}^{(k)} - \eta)^2$$

$$= \left(x^{(k)}\right)^2 + \left(tl^{(k)}{n_y}^{(k)}\right)^2 + \xi^2 - 2x^{(k)}tl^{(k)}{n_y}^{(k)} - 2x^{(k)}\xi + 2tl^{(k)}{n_y}^{(k)}\xi + (y^{(k)})^2 + (tl^{(k)}{n_x}^{(k)})^2 + \eta^2 + 2y^{(k)}tl^{(k)}{n_x}^{(k)} - 2y^{(k)}\eta - 2tl^{(k)}{n_x}^{(k)}\eta$$

$$= [\left(tl^{(k)}{n_y}^{(k)}\right)^2 + (tl^{(k)}{n_x}^{(k)})^2] + [-2x^{(k)}tl^{(k)}{n_y}^{(k)} + 2tl^{(k)}{n_y}^{(k)}\xi + 2y^{(k)}tl^{(k)}{n_x}^{(k)} - 2tl^{(k)}{n_x}^{(k)}\eta] + [\left(x^{(k)} - \xi\right)^2 + \left(y^{(k)} - \eta\right)^2]$$

$$= t^2\left(l^{(k)}\right)^2\left[\left({n_y}^{(k)}\right)^2 + \left({n_X}^{(k)}\right)^2\right] + [-2tl^{(k)}{n_y}^{(k)}\left(x^{(k)} - \xi\right) + 2tl^{(k)}{n_x}^{(k)}\left(y^{(k)} - \eta\right) + [\left(x^{(k)} - \xi\right)^2 + \left(y^{(k)} - \eta\right)^2]$$

$$= t^2\left(l^{(k)}\right)^2 + 2l^{(k)}[-{n_y}^{(k)}\left(x^{(k)} - \xi\right) + {n_x}^{(k)}\left(y^{(k)} - \eta\right)]t + [\left(x^{(k)} - \xi\right)^2 + \left(y^{(k)} - \eta\right)^2]$$

$$= A^{(k)}t^2 + B^{(k)}(\xi,\eta)t + E^{(k)}(\xi,\eta)$$

Here,

$$A^{(k)} = [l^{(k)}]^2$$

$$B^{(k)}(\xi,\eta) = [-{n_y}^{(k)}\left(x^{(k)} - \xi\right) + {n_x}^{(k)}\left(y^{(k)} - \eta\right)](2l^{(k)})$$

$$E^{(k)}(\xi,\eta) = \left(x^{(k)} - \xi\right)^2 + \left(y^{(k)} - \eta\right)^2 \tag{2.41}$$

For any point(ξ,η), the parameter $4A^{(k)}E^{(k)}(\xi,\eta) - \left[B^{(k)}(\xi,\eta)\right]^2 \geq 0$. To prove it is true, we will assume a straight line which is defined by parametric equations defined by $x = \mathrm{x}^{(k)} - tl^{(k)}{n_y}^{(k)}$ and $y = \mathrm{y}^{(k)} + tl^{(k)}{n_x}^{(k)}$ for $-\infty < t < \infty$. $C^{(k)}$ is a subset of the straight line specified in the parametric equations from $t = 0\ to\ t = 1$. Equation (2.40) holds true for any point (x, y) which is lying on the extended line. In case where (ξ,η) does not lie on the line then $A^{(k)}t^2 + B^{(k)}(\xi,\eta)t + E^{(k)}(\xi,\eta) > 0$ for all t $\in R$ (real values) (that is for all the points (x, y) on the line) and hence $4A^{(k)}E^{(k)}(\xi,\eta) - \left[B^{(k)}(\xi,\eta)\right]^2 > 0$. Another case when (ξ,η) is on the line, we can only get one point (x, y) for which the equation $A^{(k)}t^2 + B^{(k)}(\xi,\eta)t + E^{(k)}(\xi,\eta) = 0$. For each point (x, y) on the line, we may deduce that $4A^{(k)}E^{(k)}(\xi,\eta) - \left[B^{(k)}(\xi,\eta)\right]^2 = 0$ for (ξ,η) lying on the line for a unique value of t. As we know from the expression (2.40) the left-hand side portion minimum value is zero as it is sum of two squares and zero is possible at the point (ξ,η).

From equations (2.34), (2.39), (2.40)

$$F_1^k(\xi,\eta) = \frac{l^{(k)}}{4\pi}\int_0^1 ln[A^{(k)}t^2 + B^{(k)}(\xi,\eta)t + E^{(k)}(\xi,\eta)]\ dt$$

$$F_2^k(\xi,\eta) = \frac{l^{(k)}}{4\pi}\int_0^1 \frac{{n_x}^{(k)}\left(x^{(k)} - \xi\right) + {n_y}^{(k)}\left(y^{(k)} - \eta\right)}{A^{(k)}t^2 + B^{(k)}(\xi,\eta)t + E^{(k)}(\xi,\eta)}dt \tag{2.42}$$

Now, we will solve the second integral of equation (2.42) for the case $4A^{(k)}E^{(k)}(\xi,\eta) - \left[B^{(k)}(\xi,\eta)\right]^2 = 0$. This case (ξ,η) lies on the straight line of which the element $C^{(k)}$ is a subset. So, the vector $[\left(x^{(k)} - \xi\right), \left(y^{(k)} - \eta\right)]$ is normal to $[{n_x}^{(k)}, {n_y}^{(k)}]$, that is ${n_x}^{(k)}\left(x^{(k)} - \xi\right) + {n_y}^{(k)}\left(y^{(k)} - \eta\right) = 0$, and we obtain

$$F_2^k(\xi,\eta) = 0 \text{ for } 4A^{(k)}E^{(k)}(\xi,\eta) - \left[B^{(k)}(\xi,\eta)\right]^2 = 0 \tag{2.43}$$

Integration formula

$$\int \frac{dt}{at^2 + bt + c} = \frac{2}{\sqrt{4ac - b^2}}\arctan\left(\frac{2at + b}{\sqrt{4ac - b^2}}\right) + constant$$

$$For\ (a, b, c) \in R \text{ such that } 4ac - b^2 > 0$$

We find that

$$F_2^k(\xi,\eta) = \frac{l^{(k)}[{n_x}^{(k)}(x^{(k)}-\xi)+{n_y}^{(k)}(y^{(k)}-\eta)]}{\pi\sqrt{4A^{(k)}E^{(k)}(\xi,\eta)-\left[B^{(k)}(\xi,\eta)\right]^2}} \times [arctan\left(\frac{2A^{(k)}+B^{(k)}(\xi,\eta)}{\sqrt{4A^{(k)}E^{(k)}(\xi,\eta)-\left[B^{(k)}(\xi,\eta)\right]^2}}\right) - arctan\left(\frac{B^{(k)}(\xi,\eta)}{\sqrt{4A^{(k)}E^{(k)}(\xi,\eta)-\left[B^{(k)}(\xi,\eta)\right]^2}}\right)] \quad \text{for } 4A^{(k)}E^{(k)}(\xi,\eta)-\left[B^{(k)}(\xi,\eta)\right]^2 > 0$$

(2.44)

If $4A^{(k)}E^{(k)}(\xi,\eta)-\left[B^{(k)}(\xi,\eta)\right]^2 = 0$ we can write

$$A^{(k)}t^2 + B^{(k)}(\xi,\eta)t + E^{(k)}(\xi,\eta) = A^{(k)}(t+\frac{B^{(k)}(\xi,\eta)}{2A^{(k)}})^2$$

$$\begin{aligned} A^{(k)}t^2 + B^{(k)}(\xi,\eta)t + E^{(k)}(\xi,\eta) &= A^{(k)}[t^2 + 2\times\frac{B^{(k)}(\xi,\eta)}{2A^{(k)}} + \left(\frac{B^{(k)}(\xi,\eta)}{2A^{(k)}}\right)^2 - \left(\frac{B^{(k)}(\xi,\eta)}{2A^{(k)}}\right)^2 + \frac{E^{(k)}(\xi,\eta)}{A^{(k)}}] \\ &= A^{(k)}\left(t+\frac{B^{(k)}(\xi,\eta)}{2A^{(k)}}\right)^2 + \left(\frac{-(B^{(k)}(\xi,\eta))^2+4A^{(k)}E^{(k)}(\xi,\eta)}{4(A^{(k)})^2}\right) \end{aligned}$$

As, $4A^{(k)}E^{(k)}(\xi,\eta)-\left[B^{(k)}(\xi,\eta)\right]^2 = 0$, $\left(\frac{-(B^{(k)}(\xi,\eta))^2+4A^{(k)}E^{(k)}(\xi,\eta)}{4(A^{(k)})^2}\right) = 0$

So, we can write

$$A^{(k)}t^2 + B^{(k)}(\xi,\eta)t + E^{(k)}(\xi,\eta) = A^{(k)}(t+\frac{B^{(k)}(\xi,\eta)}{2A^{(k)}})^2$$

Thus, we can write,

$$F_1^k(\xi,\eta) = \frac{l^{(k)}}{4\pi}\int_0^1 \ln[A^{(k)}(t+\frac{B^{(k)}(\xi,\eta)}{2A^{(k)}})^2]\ \mathrm{dt} \qquad \text{for} \quad 4A^{(k)}E^{(k)}(\xi,\eta)-\left[B^{(k)}(\xi,\eta)\right]^2 = 0$$

(2.45)

When (ξ,η) point will lie on smoother part of $C^{(k)}$ then as per equation (2.40) $A^{(k)}t^2 + B^{(k)}(\xi,\eta)t + E^{(k)}(\xi,\eta) = 0$, while solving this equation using Sridhar Acharya formula and using equation (2.45) as $4A^{(k)}E^{(k)}(\xi,\eta)-\left[B^{(k)}(\xi,\eta)\right]^2 = 0$, we can get the solution of equation $A^{(k)}t^2 + B^{(k)}(\xi,\eta)t + E^{(k)}(\xi,\eta) = 0$, is $t = t_0 \equiv -B^{(k)}(\xi,\eta)/(2A^{(k)}) \in (0,1)$. As, we can find that at this point integrand is not well defined. So, we try to evaluate integral by using Cauchy principal sense, for this instead of [0,1] we will integrate over $[0, t_0-\varepsilon] \cup [t_0+\varepsilon, 1]$ and then let $\varepsilon \to 0$ to get its value. However, it turns out that integration limits t=$t_0-\varepsilon$ and t=$t_0+\varepsilon$ eventually contribute nothing to this integral in this situation. As a result, for $4A^{(k)}E^{(k)}(\xi,\eta)-\left[B^{(k)}(\xi,\eta)\right]^2 = 0$ the final analytic formula for $F_1^k(\xi,\eta)$ is the same regardless of whether (ξ,η) lies on $C^{(k)}$we may ignore the behaviour of the integrand and use the fundamental theorem of the integral calculus to calculate the definite integral in equation (2.45) directly over [0,1]

We know the integration formula

$\int \ln x\, dx = x(\ln x - 1) + C$, where C is constant of integration.

Now, we try to use it in definite integral sense

$$F_1^k(\xi,\eta) = \frac{l^{(k)}}{4\pi}\int_0^1 ln[A^{(k)}(t + \frac{B^{(k)}(\xi,\eta)}{2A^{(k)}})^2]\ dt$$

$$= \frac{l^{(k)}}{4\pi}\int_0^1 ln\, A^{(k)} dt + \frac{l^{(k)}}{2\pi}\int_0^1 ln\left(t + \frac{B^{(k)}(\xi,\eta)}{2A^{(k)}}\right)dt$$

$$\frac{l^{(k)}}{4\pi}\int_0^1 ln\, A^{(k)} dt = \frac{l^{(k)}}{4\pi} ln\, A^{(k)}$$

Using equation (2.41) $A^{(k)} = [l^{(k)}]^2$

$$\frac{l^{(k)}}{4\pi}\int_0^1 ln\, A^{(k)} dt = \frac{l^{(k)}}{4\pi} ln\, A^{(k)} = \frac{l^{(k)}}{2\pi} ln\, l^{(k)}$$

Now, let us assume

$$\left(t + \frac{B^{(k)}(\xi,\eta)}{2A^{(k)}}\right) = x$$

So, $dt = dx$

So, the integration limit will change

$$\frac{l^{(k)}}{2\pi}\int_0^1 ln\left(t + \frac{B^{(k)}(\xi,\eta)}{2A^{(k)}}\right)dt = \frac{l^{(k)}}{2\pi}\int_{\frac{B^{(k)}(\xi,\eta)}{2A^{(k)}}}^{(1+\frac{B^{(k)}(\xi,\eta)}{2A^{(k)}})} ln\, x\ \ dx = \frac{l^{(k)}}{2\pi}[x\, ln\, x - x]_{\frac{B^{(k)}(\xi,\eta)}{2A^{(k)}}}^{(1+\frac{B^{(k)}(\xi,\eta)}{2A^{(k)}})}$$

$$= \left(1 + \frac{B^{(k)}(\xi,\eta)}{2A^{(k)}}\right) ln\left(1 + \frac{B^{(k)}(\xi,\eta)}{2A^{(k)}}\right) - \frac{B^{(k)}(\xi,\eta)}{2A^{(k)}} ln(\frac{B^{(k)}(\xi,\eta)}{2A^{(k)}}) - 1$$

Finally, we can get

$$F_1^k(\xi,\eta) = \frac{l^{(k)}}{4\pi}\{ln(\, l^{(k)}) + (1 + \frac{B^{(k)}(\xi,\eta)}{2A^{(k)}})\, ln\left|1 + \frac{B^{(k)}(\xi,\eta)}{2A^{(k)}}\right| - \frac{B^{(k)}(\xi,\eta)}{2A^{(k)}} ln\left|\frac{B^{(k)}(\xi,\eta)}{2A^{(k)}}\right| - 1\}$$

For $4A^{(k)}E^{(k)}(\xi,\eta) - \left[B^{(k)}(\xi,\eta)\right]^2 = 0$ (2.46)

Using the integration formula

$$\int \ln(at^2 + bt + c)dt = t[\ln(a) - 2] + (t + \frac{b}{2a})\ln[t^2 + \frac{b}{a}t + \frac{c}{a}] + \frac{1}{a}\sqrt{4ac - b^2}\arctan\left(\frac{2at+b}{\sqrt{4ac-b^2}}\right) + constant$$

For real numbers a, b, c such that $\sqrt{4ac - b^2} > 0$,

we obtain

$$F_1^k(\xi,\eta) = \frac{l^{(k)}}{4\pi}\Big\{2\,ln[(l^{(k)}) - 1] - \frac{B^{(k)}(\xi,\eta)}{2A^{(k)}}\,ln\left|\frac{E^{(k)}(\xi,\eta)}{A^{(k)}}\right| + \left(1 + \frac{B^{(k)}(\xi,\eta)}{2A^{(k)}}\right)ln\left|1 + \frac{B^{(k)}(\xi,\eta)}{A^{(k)}} + \frac{E^{(k)}(\xi,\eta)}{A^{(k)}}\right| + \frac{\sqrt{4A^{(k)}E^{(k)}(\xi,\eta) - [B^{(k)}(\xi,\eta)]^2}}{A^{(k)}} \times [arctan\left(\frac{2A^{(k)} + B^{(k)}(\xi,\eta)}{\sqrt{4A^{(k)}E^{(k)}(\xi,\eta) - [B^{(k)}(\xi,\eta)]^2}}\right) - arctan\left(\frac{B^{(k)}(\xi,\eta)}{\sqrt{4A^{(k)}E^{(k)}(\xi,\eta) - [B^{(k)}(\xi,\eta)]^2}}\right)]\Big\}$$

For $4A^{(k)}E^{(k)}(\xi,\eta) - \left[B^{(k)}(\xi,\eta)\right]^2 > 0$ (2.47)

Thus, we have attained the formulae of constant boundary elements for solving Laplace equation. Now we will validate this with a numeric problem.

2.6 Numerical implementation of Laplace type problem

To validate the Fortran77 program prepared to solve Laplace problems using constant elements, we now solve a simple heat flow potential problem as described next. We analyze a square shaped close domain shown in figure 2.6. Initially we divide each arm of the boundary into 3 constant elements, i.e., 12 elements overall, and increase number of elements subsequently for mesh convergence study. Top and bottom horizontal surface flux is specified as zero and left and right vertical surfaces potential is specified.

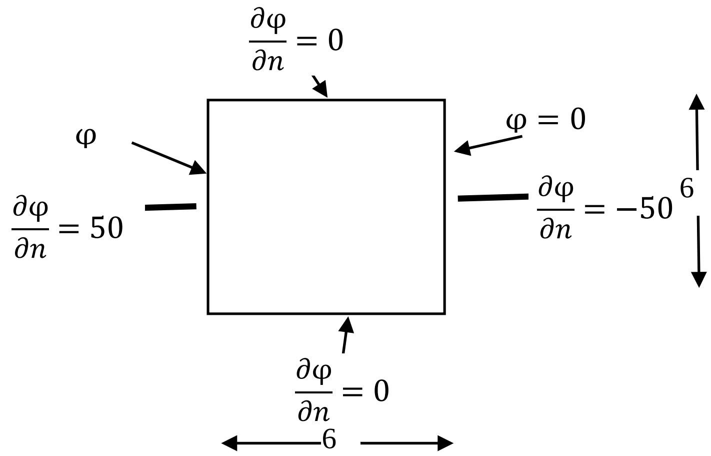

(a) Problem definition

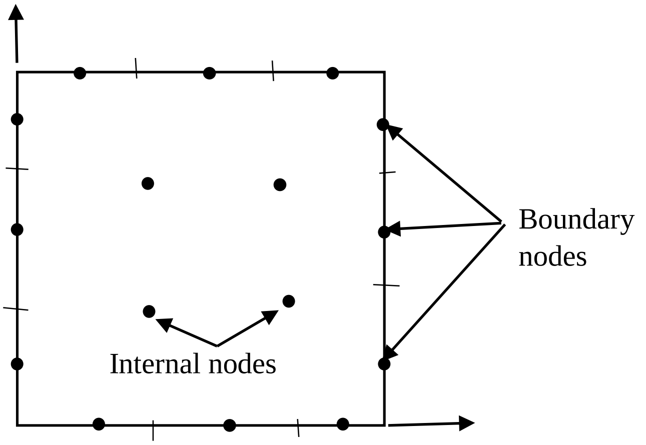

(b) Boundary elements discretization

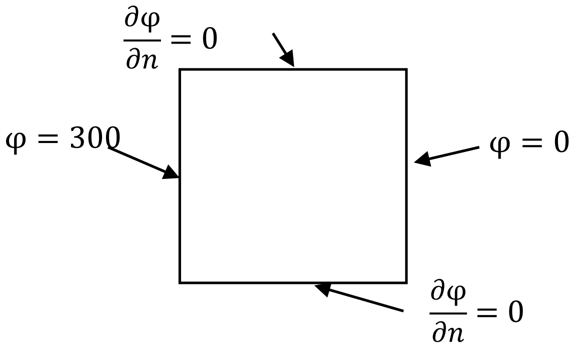

(c) Boundary conditions

Figure 2.6: Simple potential problem

Exact solution results are shown in figure (2.6a) as potential left vertical portion is 300 and right vertical boundary is 0. They are spaced at distance 6 units. So, flux will be $\frac{300}{6} = 50$. It is the exact solution.

We can analytically find out the potential value at internal points. Potential drops 300 to 0 in 6m interval. So, it drops $(300/6 = 50)$ per unit length. So, internal node at point (2,4) and (2,2) it drops potential value $\frac{300\times2}{6}$. So, potential value of these points will be $(300 - \frac{300\times2}{6}) = 200$. Similarly, at internal points (4,2) and (4,2) analytical potential value will be $(300 - \frac{300\times4}{6}) = 100$

OUTPUT FILE (for **12 number** of boundary nodes)

(BCT=0, φ specified BCT=1, $\frac{\partial \varphi}{\partial n}$ specified)

```
COORDINATES OF EXTREME POINTS OF THE BOUNDARY ELEMENTS
i          xb          yb       bct      bcv
  1     0.000000     0.000000    1     0.000000
  2     2.000000     0.000000    1     0.000000
  3     4.000000     0.000000    1     0.000000
  4     6.000000     0.000000    0     0.000000
  5     6.000000     2.000000    0     0.000000
  6     6.000000     4.000000    0     0.000000
  7     6.000000     6.000000    1     0.000000
  8     4.000000     6.000000    1     0.000000
  9     2.000000     6.000000    1     0.000000
 10      0.000000     6.000000    0    300.000000
 11      0.000000     4.000000    0    300.000000
 12      0.000000     2.000000    0    300.000000
```

```
BOUNDARY NODES
  i          xm          ym
  1     1.000000     0.000000
  2     3.000000     0.000000
```

```
   3      5.000000      0.000000
   4      6.000000      1.000000
   5      6.000000      3.000000
   6      6.000000      5.000000
   7      5.000000      6.000000
   8      3.000000      6.000000
   9      1.000000      6.000000
  10       0.000000      5.000000
  11       0.000000      3.000000
  12       0.000000      1.000000
  13       2.000000      2.000000
  14       2.000000      4.000000
  15       4.000000      2.000000
  16       4.000000      4.000000
```

```
Boundary      x              y            c_phi            z            c_dphi
 ------------------------------------------------------------------------------------------
   1       1.000000       0.000000     252.261806       0.000000     252.261806
   2       3.000000       0.000000     150.000000       0.000000     150.000000
   3       5.000000       0.000000      47.738194       0.000000      47.738194
   4       6.000000       1.000000       0.000000     -52.954412     -52.954412
   5       6.000000       3.000000       0.000000     -48.761501     -48.761501
   6       6.000000       5.000000       0.000000     -52.954412     -52.954412
   7       5.000000       6.000000      47.738194       0.000000      47.738194
   8       3.000000       6.000000     150.000000       0.000000     150.000000
   9       1.000000       6.000000     252.261806       0.000000     252.261806
  10       0.000000       5.000000     300.000000      52.954412      52.954412
  11       0.000000       3.000000     300.000000      48.761501      48.761501
  12       0.000000       1.000000     300.000000      52.954412      52.954412
```

```
Internal        x              y          Numerical phi
 ---------------------------------------------------
  13       2.000000       2.000000     200.268946
  14       2.000000       4.000000     200.268946
  15       4.000000       2.000000      99.731054
  16       4.000000       4.000000      99.731054
```

Values at nodes 4, 5, 6, 10, 11, and 12 are closest to the exact value of $\frac{\partial\varphi}{\partial n}$.

Values at internal nodes at 13,14,15 and 16 are closest to the exact value of φ

Table 2.1a: Percentage error of boundary nodes for **12** number of boundary elements

Internal Boundary Node	Flux from Numerical Analysis	Flux from Analytical value	% Error
5	-48.76151501	-50	2.47697
11	48.761501	50	2.476998

Table 2.1b: Percentage error of internal nodes for **12** number of boundary elements

Internal Node	Potential from Numerical Analysis	Potential from Analytical value	% Error
13	200.268946	200	0.134473
14	200.268946	200	0.134473
15	99.731054	100	0.268946
16	99.731054	100	0.268946

We now run the process with **16** boundary elements

```
OUTPUT FILE
Boundary     x          y            c_phi             z             c_dphi
 -------------------------------------------------
    1       0.750000      0.000000     264.369666      0.000000     264.369666
    2       2.250000      0.000000     188.031890      0.000000     188.031890
    3       3.750000      0.000000     111.968110      0.000000     111.968110
    4       5.250000      0.000000      35.630334      0.000000      35.630334
    5       6.000000      0.750000       0.000000    -52.761446    -52.761446
    6       6.000000      2.250000       0.000000    -49.208334    -49.208334
    7       6.000000      3.750000       0.000000    -49.208334    -49.208334
    8       6.000000      5.250000       0.000000    -52.761446    -52.761446
    9       5.250000      6.000000      35.630334      0.000000      35.630334
   10       3.750000      6.000000     111.968110      0.000000     111.968110
   11       2.250000      6.000000     188.031890      0.000000     188.031890
   12       0.750000      6.000000     264.369666      0.000000     264.369666
   13       0.000000      5.250000     300.000000     52.761446      52.761446
   14       0.000000      3.750000     300.000000     49.208334      49.208334
   15       0.000000      2.250000     300.000000     49.208334      49.208334
   16       0.000000      0.750000     300.000000     52.761446      52.761446
 Internal       x         y           Numerical phi
 -------------------------------------------------
   17       2.000000      2.000000     200.179648
   18       2.000000      4.000000     200.179648
   19       4.000000      2.000000      99.820352
   20       4.000000      4.000000      99.820352
```

Table 2.2a: Percentage error of boundary nodes for **16** number of boundary elements

Interior Boundary Node	Flux from Numerical Analysis	Flux from Analytical value	% Error
6	-49.208334	-50	1.583332
7	-49.208334	-50	1.583332
14	49.208334	50	1.583332
15	49.208334	50	1.583332

Table 2.2b: Percentage error of internal nodes for **16** number of boundary elements

Internal Node	Potential from Numerical Analysis	Potential from Analytical value	% Error
17	200.179648	200	0.089824
18	200.179648	200	0.089824
19	99.820352	100	0.179648
20	99.820352	100	0.179648

Finally, we use **20 number** of boundary elements:

```
OUTPUT FILE
Boundary      x           y              c_phi              z              c_dphi
 -------------------------------------------------
    1      0.600000     0.000000    271.569541     0.000000    271.569541
    2      1.800000     0.000000    210.642898     0.000000    210.642898
    3      3.000000     0.000000    150.000000     0.000000    150.000000
    4      4.200000     0.000000     89.357102     0.000000     89.357102
    5      5.400000     0.000000     28.430459     0.000000     28.430459
    6      6.000000     0.600000      0.000000   -52.660270   -52.660270
    7      6.000000     1.800000      0.000000   -49.188984   -49.188984
    8      6.000000     3.000000      0.000000   -49.744772   -49.744772
    9      6.000000     4.200000      0.000000   -49.188984   -49.188984
   10      6.000000     5.400000      0.000000   -52.660270   -52.660270
   11      5.400000     6.000000     28.430459     0.000000     28.430459
   12      4.200000     6.000000     89.357102     0.000000     89.357102
   13      3.000000     6.000000    150.000000     0.000000    150.000000
   14      1.800000     6.000000    210.642898     0.000000    210.642898
   15      0.600000     6.000000    271.569541     0.000000    271.569541
   16      0.000000     5.400000    300.000000    52.660270     52.660270
   17      0.000000     4.200000    300.000000    49.188983     49.188983
   18      0.000000     3.000000    300.000000    49.744773     49.744773
   19      0.000000     1.800000    300.000000    49.188983     49.188983
   20      0.000000     0.600000    300.000000    52.660270     52.660270

Internal       x          y            Numerical phi
 -------------------------------------------------
   21      2.000000     2.000000    200.133309
   22      2.000000     4.000000    200.133309
   23      4.000000     2.000000     99.866691
   24      4.000000     4.000000     99.866691
```

Table 2.3a: Percentage error of boundary nodes for **20** number of boundary elements

Interior Boundary Node	Flux from Numerical Analysis	Flux from Analytical value	% Error
8	-49.744772	-50	0.510456
18	49.744773	50	0.510454

Table 2.3b: Percentage error of internal nodes for **20** number of boundary elements

Internal Node	Potential from Numerical Analysis	Potential from Analytical value	% Error
21	200.133309	200	0.066645
22	200.133309	200	0.0666545
23	99.866691	100	0.133309
24	99.866691	100	0.133309

Results and Discussions

From the above discussions, it is clearly evident that as we refine the number of boundary elements from 12 to 20, the solution monotonically converged to the exact solution. So, our numerical formulation of Laplace equation is validated.

Up to this we have discussed boundary element formulation for Laplace equation. Now, we will extend it to solve dual reciprocity BEM for non-homogeneous Helmholtz type equation problems. In Dual Reciprocity BEM we will use the fundamental solution of simpler Laplace equation to solve the Helmholtz type equation and we will use constant elements for computational purpose. So, these formulas for constant elements to evaluate functions $F_1^k(\xi, \eta)$ and $F_2^k(\xi, \eta)$ will also be used for solving Helmholtz equation.

Chapter 3

The Dual Reciprocity Boundary Element Formulation

3.1 The Generalized Helmholtz Equation with Variable Coefficients

It has been mentioned earlier that the Generalized Helmholtz equations are visible in multiple engineering problems like acoustics, seismology, heat transfer and mechanics of inhomogeneous bodies. Thus, if a generalized boundary integral formulation is made available that addresses all such problems, it would be a lucrative proposal and the thesis has thrived at this only but delimited to two-dimensional domains and constant elements only due to time constraints. To understand the dual reciprocity boundary element method, we take the help of references [11, 12, 14, and 15]. Here in this chapter, we will discuss step by step the procedure of dual reciprocity boundary element formulation.

The generalized Helmholtz equation with variable coefficients may be expressed as

$$\frac{\partial^2\varphi}{\partial x^2}+\frac{\partial^2\varphi}{\partial y^2}+\alpha(x,y)\varphi = g(x,y) \tag{3.1}$$

Valid in a two-dimensional region R bounded by a simple closed curve C. Usually, the boundary is subject to the following 'boundary conditions':

A) The "Essential" boundary condition

$\varphi = f_1(x,y)$ for $(x,y) \in C_1$, and

B) The "Natural" boundary condition

$\frac{\partial\varphi}{\partial n}= f_2(x,y)$ for $(x,y) \in C_2$.

(3.2)

It could often difficult be to obtain a generalized fundamental solution for equation (3.1) if the coefficients $\alpha(x,y)$ and $g(x,y)$ vary smoothly over the space. However, still a BIE can be derived using the fundamental solution for the two-dimensional Laplace equation (ref. equation 2.14), as given below

$$\Phi(x,y;\xi,\eta) = \frac{1}{4\pi}ln((x-\xi)^2+(y-\eta)^2) \tag{3.3}$$

with (x,y) the field point and (ξ,η) the source point, or vice versa.

Let's assume that there are two potential functions, φ_1 and φ_2, which satisfy the following Poisson equations for our region of interest R bounded by a simple closed curve C

$$\frac{\partial^2\varphi_1}{\partial x^2}+\frac{\partial^2\varphi_1}{\partial y^2} = \sigma_1 \tag{3.4a}$$

$$\frac{\partial^2\varphi_2}{\partial x^2}+\frac{\partial^2\varphi_2}{\partial y^2} = \sigma_2 \tag{3.4b}$$

If we multiply equation (3.4a) by φ_2 and equation (3.4b) by φ_1, we obtain

$$\varphi_2\frac{\partial^2\varphi_1}{\partial x^2}+\varphi_2\frac{\partial^2\varphi_1}{\partial y^2} = \varphi_2\sigma_1$$

$$\varphi_1 \frac{\partial^2 \varphi_2}{\partial x^2} + \varphi_1 \frac{\partial^2 \varphi_2}{\partial y^2} = \varphi_1 \sigma_2$$

Taking their difference, we find

$$\varphi_2 \frac{\partial^2 \varphi_1}{\partial x^2} - \varphi_1 \frac{\partial^2 \varphi_2}{\partial x^2} + \varphi_2 \frac{\partial^2 \varphi_1}{\partial y^2} - \varphi_1 \frac{\partial^2 \varphi_2}{\partial y^2} = \varphi_2 \sigma_1 - \varphi_1 \sigma_2$$

Or, $\varphi_2 \sigma_1 - \varphi_1 \sigma_2 = \varphi_2 \frac{\partial^2 \varphi_1}{\partial x^2} - \varphi_1 \frac{\partial^2 \varphi_2}{\partial x^2} + \varphi_2 \frac{\partial^2 \varphi_1}{\partial y^2} - \varphi_1 \frac{\partial^2 \varphi_2}{\partial y^2}$

Integrating above equation over the domain R, we obtain

$$\iint_R \left[\varphi_2 \sigma_1 - \varphi_1 \sigma_2\right] dR = \iint_R \left[\varphi_2 \nabla^2 \varphi_1 - \varphi_1 \nabla^2 \varphi_2\right] dR$$

Applying Gauss divergence theorem (Refer equation (A.20) to the right-hand side of above expression one obtains

$$\iint_R \left[\varphi_2 \sigma_1 - \varphi_1 \sigma_2\right] dx\, dy = \int_C \left[\varphi_2 \frac{\partial \varphi_1}{\partial n} - \varphi_1 \frac{\partial \varphi_2}{\partial n}\right] ds(x, y)$$

Changing sides, we have

$$\int_C \left(\varphi_2 \frac{\partial \varphi_1}{\partial n} - \varphi_1 \frac{\partial \varphi_2}{\partial n}\right) ds(x, y) = \iint_R (\varphi_2 \sigma_1 - \varphi_1 \sigma_2) dx\, dy \qquad (3.5)$$

It may be noted here that equation (3.5) demands that σ_1 and σ_2 be any two such expressions that renders the expression $\varphi_2\sigma_1 - \varphi_1\sigma_2$ integrable over region R.

Equation (3.5) is employed to derive an integral equation for the generalized Helmholtz equation (3.1). For this, let's visualize φ_1 as the fundamental solution of two-dimensional Laplace's equation, i.e., $\varphi_1 = \Phi(x, y; \xi, \eta)$ that is defined in equation (3.3) while φ_2 is envisioned as the coveted solution of equation (3.1) given the boundary condition equation (3.2). Let's then set $\varphi_2 = \varphi$. In equations (3.4), we have thus set, $\sigma_1 = 0$ and $\sigma_2 = g(x, y) - \alpha(x, y)\varphi$.

We can rewrite left hand side of equation (3.5) after substituting $\varphi_1 = \Phi(x, y; \xi, \eta)$, $\varphi_2 = \varphi(x, y)$

$$\int_C \left(\varphi_2 \frac{\partial \varphi_1}{\partial n} - \varphi_1 \frac{\partial \varphi_2}{\partial n}\right) ds(x, y) = \int_C \left(\varphi(x, y) \frac{\partial \Phi(x, y; \xi, \eta)}{\partial n} - \Phi(x, y; \xi, \eta) \frac{\partial \varphi(x, y)}{\partial n}\right) ds(x, y)$$

Let's consider a point (ξ, η) that lies inside region R. Now we revert back to section 2.3 where direct BEM formulation for Laplace equation is discussed. From our detailed discussion in section 2.3, we get the general boundary integral equation [equation (2.30)] in the form

$$\lambda(\xi, \eta)\, \varphi(\xi, \eta) = \int_C \left(\varphi(x, y) \frac{\partial \Phi(x, y; \xi, \eta)}{\partial n} - \Phi(x, y; \xi, \eta) \frac{\partial \varphi(x, y)}{\partial n}\right) ds(x, y) \qquad (2.30)$$

Now, we compare with equation (3.5) with equation (2.30). We can clearly see that left hand side of equation (3.5) is similar with right hand side of equation (2.30). So, we can rewrite equation (3.5) after adjusting right hand side double integration tern of equation (3.5) as below

$$\lambda(\xi,\eta)\varphi(\xi,\eta)-\iint_R \Phi(x,y;\xi,\eta)[g(x,y)-\alpha(x,y)\varphi(x,y)]\,dx\,dy$$
$$=\int_C \left(\varphi(x,y)\frac{\partial\Phi(x,y;\xi,\eta)}{\partial n}-\Phi(x,y;\xi,\eta)\frac{\partial\varphi(x,y)}{\partial n}\right)ds(x,y)$$
$$\text{for } (\xi,\eta)\in R\cup C \qquad (3.6)$$

where,

$\lambda(\xi,\eta)=1$ for $(\xi,\eta)\in R$
$=\frac{1}{2}$ for (ξ,η) on smooth part of the boundary C
$=0$ for (ξ,η) outside R

Equation (3.6) contains a double integral over the entire solution domain R with the usual line integral over boundary C. The unknown function φ also appears in the integrand of the domain integral. We may discretize R into number of smaller domain elements to calculate double integral. But discretization of R into domain integrals can be avoided if we apply dual reciprocity method to convert double integral into a line integral over C.

3.2 Approximate of domain integral

Let's define a radial basis function, ρ, centred about the point (a,b) as a function of the form $\rho(x,y;a,b)=G(r(x,y;a,b))$, where $r(x,y;a,b)=\sqrt{(x-a)^2+(y-a)^2}$,so that $\rho(x,y;a,b)$ is dependent only on the distance of point (x,y) from point (a,b)

Let ρ be defined as

$$\rho(x,y;a,b)=1+r^2(x,y;a,b)+r^3(x,y;a,b) \qquad (3.7)$$

We now approximate $[g(x,y)-\alpha(x,y)\varphi(x,y)]$ using the radial basis functions of the form given in equation (3.7) centred about M number of points selected in $R\cup C$. Selected points are given by $(a^{(1)},b^{(1)})$, $(a^{(2)},b^{(2)}),\cdots,$ $(a^{(M-1)},b^{(M-1)})$, $(a^{(M)},b^{(M)})$, then we can make following assumption

$$[g(x,y)-\alpha(x,y)\varphi(x,y)]\cong\sum_{m=1}^{M}\beta^{(m)}\rho(x,y;a^{(m)},b^{(m)}) \qquad (3.8)$$

where we have to evaluate the M coefficients $\beta^{(m)}$ $m=1,\dots,M$. For better results the M points that we select should be well-dispersed in R and some of them could also be positioned on the boundary C.

$$\iint_R \Phi(x,y;\xi,\eta)[g(x,y)-\alpha(x,y)\varphi(x,y)]dxdy$$

$$\cong\sum_{m=1}^{M}\beta^{(m)}\iint_R \Phi(x,y;\xi,\eta)\,\rho\big(x,y;a^{(m)},b^{(m)}\big)\,dxdy \qquad (3.9)$$

Let's introduce a function $\chi(x,y;a,b)$ such that

$$\frac{\partial^2\chi}{\partial x^2}+\frac{\partial^2\chi}{\partial y^2}=\rho \qquad (3.10)$$

Then we again apply *reciprocal relation* in equation (3.5) with $\varphi_1=\Phi(x,y;\xi,\eta)$, $\varphi_2=\chi(x,y;a,b)$. $\sigma_1=0$ and $\sigma_2=\rho(x,y;a,b)$, From equation (3.6) we can get

$$\lambda(\xi,\eta)\chi(\xi,\eta;a,b) - \iint_R \Phi(x,y;\xi,\eta)\ \rho(x,y;a,b)\ dxdy$$

$$= \int_C \left[\chi(x,y;a,b)\frac{\partial\Phi(x,y;\xi,\eta)}{\partial n} - \Phi(x,y;\xi,\eta)\frac{\partial\chi(x,y;a,b)}{\partial n}\right] ds(x,y)$$

Rearranging we get

$$\iint_R \Phi(x,y;\xi,\eta)\ \rho(x,y;a,b)dxdy = \lambda(\xi,\eta)\chi(\xi,\eta;a,b) + \int_C \left[\Phi(x,y;\xi,\eta)\frac{\partial\chi(x,y;a,b)}{\partial n} - \chi(x,y;a,b)\frac{\partial\Phi(x,y;\xi,\eta)}{\partial n}\right]ds(x,y)$$

We assume a function $\Psi(\xi,\eta;a,b)$ such that

$$\iint_R \Phi(x,y;\xi,\eta)\ \rho(x,y;a,b)dxdy = \Psi(\xi,\eta;a,b) \qquad (3.11)$$

So, we can write

$$\Psi(\xi,\eta;a,b) = \lambda(\xi,\eta)\chi(\xi,\eta;a,b) + \int_C \left[\Phi(x,y;\xi,\eta)\frac{\partial\chi(x,y;a,b)}{\partial n} - \chi(x,y;a,b)\frac{\partial\Phi(x,y;\xi,\eta)}{\partial n}\right]ds(x,y) \qquad (3.12)$$

If we assume that $\chi(x,y;a,b)$ is a radial basis function which is cantered about (a,b) that is,

If $\chi(x,y;a,b) = q(r)$, where $r = \sqrt{(x-a)^2 + (y-a)^2}$, equation (3.10) with equation (3.7) we can write in polar coordinates (Refer equation (A.3) where q is independent of θ means q is only function of r)

$$\frac{1}{r}\ \frac{\partial}{\partial r}\left(r\ \frac{\partial q}{\partial r}\right) = 1 + r^2 + r^3$$

If we integrate twice and set integral constant equal to zero, we can get

$$q(r) = \frac{1}{4}r^2 + \frac{1}{16}r^4 + \frac{1}{25}r^5$$

So, a possible function $\chi\ (x,y;a,b)$ is given by

$$\chi\ (x,y;a,b) = \frac{1}{4}r(x,y;a,b)^2 + \frac{1}{16}r(x,y;a,b)^4 + \frac{1}{25}r(x,y;a,b)^5 \qquad (3.13)$$

Using equation (3.13) we can write the double integral in equation (3.11) $\Psi(\xi,\eta;a,b)$ as defined in equation (3.11) can be computed by calculating a line integral with a known integrand over C. Line C can be discretized into a number of straight-line segments to approach the line integral.

Let (x,y) in equation (3.8) be given in turn by selected points by $(a^{(1)},b^{(1)})$, $(a^{(2)},b^{(2)})$, ⋯, $(a^{(M-1)},b^{(M-1)})$, $(a^{(M)},b^{(M)})$, then we can generate M number of equations

$$g\left(a^{(j)},b^{(j)}\right) - \alpha\left(a^{(j)},b^{(j)}\right)\varphi\left(a^{(j)},b^{(j)}\right) \cong \sum_{m=1}^{M}\beta^{(m)}\rho(\mathrm{x},\mathrm{y};a^{(m)},b^{(m)})$$
$$for\ j = 1,2,\ldots\ldots,M.$$

After inversion we can get

$$\beta^{(m)} = \sum_{j=1}^{M}\omega^{(mj)}\left[g\left(a^{(j)},b^{(j)}\right) - \alpha\left(a^{(j)},b^{(j)}\right)\varphi\left(a^{(j)},b^{(j)}\right)\right] \text{ for } m = 1,2,\ldots\ldots,M. \qquad (3.14)$$

Where $\omega^{(mj)}$ can be defined as

$$\sum_{j=1}^{M}\omega^{(kj)}\,\rho(a^{(j)},b^{(j)};a^{(m)},b^{(m)}) = \begin{cases} 1, & if\ \ k=m \\ 0, & if\ \ k\neq m \end{cases} \tag{3.15}$$

That is if $\rho(a^{(j)},b^{(j)};a^{(m)},b^{(m)})$ is the element of j-th row and m-th column of the square matrix **Q** then $\omega^{(kj)}$ is the element in k-th row and j-th element of $\boldsymbol{Q^{-1}}$

From equations (3.9), (3.11) and (3.14), we can write

$$\iint_R \Phi(x,y;\xi,\eta)[g(x,y)-\alpha(x,y)\varphi(x,y)]dxdy \cong \sum_{j=1}^{M}\left[g\left(a^{(j)},b^{(j)}\right) - \alpha\left(a^{(j)},b^{(j)}\right)\varphi\left(a^{(j)},b^{(j)}\right)\right]\sum_{m=1}^{M}\omega^{(mj)}\,\Psi\left(\xi,\eta;a^{(m)},b^{(m)}\right) \tag{3.16}$$

3.3 Dual-reciprocity Boundary Element Method

Using equation (3.16) we can rewrite equation (3.6) as

$$\begin{aligned}\lambda(\xi,\eta)\varphi(\xi,\eta) - \sum_{j=1}^{M}\Big[g\left(a^{(j)},b^{(j)}\right) & \\ - \alpha\left(a^{(j)},b^{(j)}\right)\varphi\left(a^{(j)},b^{(j)}\right)\Big] & \sum_{m=1}^{M}\omega^{(mj)}\,\Psi\left(\xi,\eta;a^{(m)},b^{(m)}\right) \\ = \int_C & \left(\varphi(x,y)\frac{\partial\Phi(x,y;\xi,\eta)}{\partial n} - \Phi(x,y;\xi,\eta)\frac{\partial\varphi(x,y)}{\partial n}\right)ds(x,y)\end{aligned}$$

$$\text{for } (\xi,\eta) \in R\cup C \tag{3.17}$$

Actually, we can see that the reciprocal relation given in equation (3.5) applied twice for the derivation of equation (3.17). First time for deriving equation (3.6) and secondly in approximately conversion of double integral to line integral over C as given in equation (3.12). A numeric solution for the boundary value problem defined by equations (3.1) and (3.2) is obtained from equation (3.17) is called dual-reciprocity boundary element solution.

Similar to Section 2.4, we may discretize boundary C into N number of straight-line segments $C^{(1)}, C^{(2)}, \ldots, C^{(N-1)}$, $C^{(N)}$and φ and $\frac{\partial\varphi}{\partial n}$ are **constant** on the boundary C, these functions are constant of the boundary elements. Specifically, our approximation can be written in this way $\varphi \cong \bar{\varphi}^{k}$ and $\frac{\partial\varphi}{\partial n} = \bar{p}^{k}$ for $(x,y) \in C^{(k)}$ $(k=1,2,\ldots,N)$

We take the first N collocation points for approximation which are midpoints of the boundary element in equation (3.16). $(M>N)$. Let, $(a^{(k)},b^{(k)}) = (\bar{x}^{(k)},\bar{y}^{(k)})$ (midpoint of $C^{(k)}$) for $k=1,2,3,\ldots.,N$. The remaining L $(M-N)$ points are in the interior of R. Equation (3.16) is then approximating as

$$\begin{aligned}\lambda(\bar{x}^{(n)},\bar{y}^{(n)})\bar{\varphi}^{n} - \sum_{j=1}^{N+L}\mu^{(nj)}\left[g(\bar{x}^{(j)},\bar{y}^{(j)}) - \alpha(\bar{x}^{(j)},\bar{y}^{(j)})\bar{\varphi}^{j}\right] & \\ = \sum_{k=1}^{N}\{\bar{\varphi}^{k}\,F_2^{k}(\bar{x}^{(n)},\bar{y}^{(n)}) - \bar{p}^{k}F_1^{k}(\bar{x}^{(n)},\bar{y}^{(n)})\} & \\ \text{for } n=1,2,\ldots\ldots..,N+L &\end{aligned} \tag{3.18}$$

where $\bar{\varphi}^{n} = (\bar{x}^{(n)},\bar{y}^{(n)})$ $(n=1,2,\ldots.,N+L)$

$$\mu^{(nj)} = \sum_{m=1}^{N+L} \omega^{(mj)}\, \Psi\left(\bar{x}^{(n)}, \bar{y}^{(n)}; \bar{x}^{(m)}, \bar{y}^{(m)}\right)$$

$$F_1^k(\xi,\eta) = \int_{C^{(k)}} \Phi(x,y;\xi,\eta)\, ds(x,y)$$
$$F_2^k(\xi,\eta) = \int_{C^{(k)}} \frac{\partial}{\partial n}[\Phi(x,y;\xi,\eta)]\, ds(x,y)$$

(3.19)

Formulae for calculating $F_1^k(\xi,\eta)$, $F_2^k(\xi,\eta)$ as in equation (3.19) are given in Section 2.5. $F_1^k(\xi,\eta)$ is computed by equations (2.46) and (2.47) and $F_2^k(\xi,\eta)$ is computed using equations (2.43) and (2.44).

We can find out Ψ as given in equation (3.12)

$$\begin{aligned}\Psi(\xi,\eta;a,b) = {} & \lambda(\xi,\eta)\chi(\xi,\eta;a,b) \\ & + \sum_{k=1}^{N} \left[n_x^{(k)} \frac{\partial(\chi(x,y;a,b))}{\partial x} + n_y^{(k)} \frac{\partial(\chi(x,y;a,b))}{\partial y}\right]\Bigg|_{(x,y)=(\bar{x}^{(k)},\bar{y}^{(k)})} \mathcal{F}_1^k(\xi,\eta) \\ & - \sum_{k=1}^{N} \chi(\bar{x}^{(k)},\bar{y}^{(k)};a,b)\mathcal{F}_2^k(\xi,\eta)\end{aligned}$$

(3.20)

Equation (3.18) constitutes a system of $N+L$ linear algebraic equations in $N+L$ unknowns. Unknowns are either $\overline{\varphi}^k$ or $\overline{p}^k$ but not the both for $k = 1,2,\dots\dots,N$ (depending upon boundary condition specified on a boundary element) and $\overline{\varphi}^{(N+j)}$ for $j = 1,2,\dots,L$ (the values of φ at L interior collocation points). We can rewrite equation (3.18) in the following form

$$\sum_{k=1}^{N+L} a^{(nk)}z^{(k)} = -\sum_{j=1}^{N+L} \mu^{(nj)}\left[g(\bar{x}^{(j)},\bar{y}^{(j)})\right] + \sum_{k=1}^{N} b^{(nk)}\ for\ n = 1,2,\dots,N+L$$

(3.21)

For $k = 1,2,\dots,N$, the coefficients $a^{(nk)}$, $b^{(nk)}$, $z^{(k)}$ can be written as

$$\begin{aligned} a^{(mk)} &= -F_1^k\left(\bar{x}^{(n)},\bar{y}^{(n)}\right) && \text{when } \varphi \text{ is specified over } C^{(k)} \\ &= F_2^k\left(\bar{x}^{(n)},\bar{y}^{(n)}\right) - \frac{1}{2}\delta^{(nk)} - \mu^{(nk)}\alpha(\bar{x}^{(k)},\bar{y}^{(k)}) && \text{when } \frac{\partial\varphi}{\partial n} \text{ is specified over } C^{(k)}\end{aligned}$$

$$\begin{aligned} b^{(nk)} &= \overline{\varphi}^k\left(-F_2^k\left(\bar{x}^{(n)},\bar{y}^{(n)}\right) + \frac{1}{2}\delta^{(nk)} + \mu^{(nk)}\alpha(\bar{x}^{(k)},\bar{y}^{(k)})\right) && \text{when } \varphi \text{ is specified over } C^{(k)} \\ &= \overline{p}^k F_1^k\left(\bar{x}^{(n)},\bar{y}^{(n)}\right) && \text{when } \frac{\partial\varphi}{\partial n} \text{ is specified over } C^{(k)}\end{aligned}$$

$$\begin{aligned} z^{(k)} &= \overline{p}^k && \text{when } \varphi \text{ is specified over } C^{(k)} \\ &= \overline{\varphi}^k && \text{when } \frac{\partial\varphi}{\partial n} \text{ is specified over } C^{(k)}\end{aligned}$$

When $j = 1,2,\dots,L$ the coefficients $a^{(n[N+j])}$ and $z^{(N+j)}$ are given by $a^{(n[N+j])} = -\delta^{(n[N+j])} - \mu^{(n[N+j])}\alpha(\bar{x}^{(N+j)},\bar{y}^{(N+j)})$

$$z^{(N+j)} = \overline{\varphi}^{(N+j)}$$

$$For\ n = 1,2,\dots\dots,N+L\ and\ m = 1,2,\dots.,N+L$$

$$\begin{aligned}\delta^{(nm)} &= 0 && \text{if } n \neq m \\ &= 1 && \text{if } n = m\end{aligned}$$

Till now we have derived dual reciprocity boundary element formulations for non-homogeneous Helmholtz type equation with variable coefficients. Now, for practical civil engineering purpose we will choose a two-dimensional acoustics problem, which satisfies two-dimensional homogeneous Helmholtz equation. From our previous general formulation, we can easily solve acoustics problem by setting non-homogeneous term $g(x, y) = 0$. Then we solve a practical numerical problem on acoustics and compare analytical solution with our numerical solution to validate our numerical formulation. After that we will solve a Poisson's equation problem as case study.

Chapter 4

Results and Discussions

4.1 Introduction

Till now we have derived the conventional direct boundary element formulation for Laplace type equation and solved a potential problem to numerically validate the code. Then we studied dual reciprocity boundary element formulation for non-homogeneous type Helmholtz equation, which is a generalised form of many engineering problems. Now we will try to solve a specific case. For this, we derive the governing equation for sinusoidal acoustics problems. Then we will solve a two-dimensional acoustics problem and validate it. Finally, we will solve a Poisson’s equation problem and compare the results with a finite difference hand computation as a basic solution and study the convergence upon mesh refinement.

4.2 The Governing Acoustic Equation

The internal restoring forces of a gas are related to the associated deformations by the equation of state. Because acoustic processes are fast, they can be regarded nearly adiabatic, and we can write the equation of state as follows, assuming the medium is a perfect gas [33].

$$\frac{P}{P_o} = \left(\frac{\rho}{\rho_o}\right)^{\gamma} \tag{4.1}$$

where $\gamma$is the ratio of the specific heats of the gas at constant pressure to that at constant volume, P and P_o are the instantaneous and ambient pressures, respectively, and ρ and ρ_o are instantaneous and ambient mass densities, respectively, of the acoustic fluid. Because acoustic disturbances are considered adiabatic, there must be no thermal energy transfer between neighbouring fluid elements. We can use Taylor's series expansion rule to link changes in pressure and density owing to acoustical disturbances, as demonstrated below.

$$P = P_o + \left(\frac{\partial P}{\partial \rho}\right)_{\rho_o} (\rho - \rho_o) + \left(\frac{\partial^2 P}{\partial \rho^2}\right)_{\rho_o} (\rho - \rho_o)^2/2 + \cdots \tag{4.2}$$

where the partial derivatives are constants computed for the fluid's adiabatic compression and expansion around its equilibrium density. Because the variations are minimal, only the first order term in $(\rho - \rho_o)$ may be kept. This results in a linear relationship between pressure fluctuations and density changes.

$$p = P - P_o = \left(\frac{\partial P}{\partial \rho}\right)_{\rho_o} (\rho - \rho_o) = B\,\frac{\rho - \rho_o}{\rho_o} = Bs \tag{4.3}$$

Where, $B = \rho_o(\partial P/\partial \rho)_{\rho_o}$ is the adiabatic bulk modulus, and $s = (\rho - \rho_o)/\rho_o$ is the condensation. 's' has relatively small numerical value. In fact, neither s nor the spatial rate of change of fluid particle displacement, $\partial \xi_{ai}/\partial x_j$, exceed the numerical value of 0.0001 for the intense noises in air, which are painful to human ear, where ξ_{ai} is the particle displacement from its equilibrium position.

The equation of continuity for the acoustic fluid may be derived with reference to Fig. 4.1, exhibiting a fixed control volume $dV = dx\,dy\,dz$ in space, through which fluid flows with velocity $\vec{u}_a$ ($\equiv \partial \xi_a/\partial t$) and instantaneous density ρ. The net mass influx into this spatially fixed volume, resulting from flow in the *x* direction, is $-\frac{\partial(\rho u_{ax})}{\partial x} dV$.

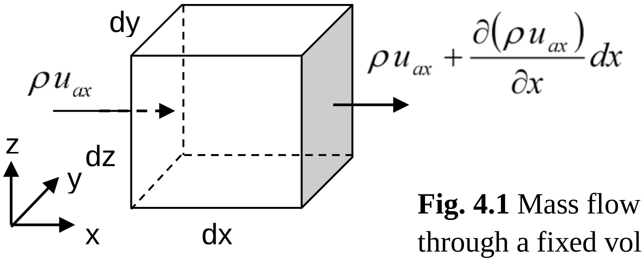

Fig. 4.1 Mass flow in the *x* direction through a fixed volume dV.

Similar expressions can be obtained for the *y* and *z* directions too, so that the total influx is

$$-\left[\frac{\partial(\rho u_{ax})}{\partial x} + \frac{\partial(\rho u_{ay})}{\partial y} + \frac{\partial(\rho u_{az})}{\partial z}\right] dV \equiv -[\nabla \cdot (\rho \vec{u}_a)]dV \tag{4.4}$$

Where, $\nabla$is the divergence operator. The rate with which the mass increases inside this volume is $(\partial \rho/\partial t)dV$. Since the net influx must equal the rate of increase, hence,

$$\frac{\partial \rho}{\partial t} + \nabla \cdot (\rho \vec{u}_a) = 0 \tag{4.5}$$

This is the equation of continuity, non-linear by nature. However, from the definition of condensation, the instantaneous mass density of air may be written as

$$\rho = \rho_o(1 + s), \tag{4.6}$$

where $\rho_o$is the constant ambient mass density and s is very small, which linearizes the non-linear equation of continuity as

$$\frac{\partial s}{\partial t} + \nabla \cdot \vec{u}_a = 0 \tag{4.7}$$

This equation can be integrated with respect to time to relate the condensation with fluid particle displacements, ξ_{ai}, as follows

$$s = -\nabla \cdot \vec{\xi}_a \tag{4.8}$$

since, $\int \nabla \cdot \vec{u}_a dt = \nabla \cdot \int \vec{u}_a dt = \nabla \cdot \int \left(\partial \vec{\xi}_a / \partial t\right) dt = \nabla \cdot \vec{\xi}_a$, and the constant of integration is zero, because the acoustic quantities are all zero if there is no disturbance present. The quantity $\vec{\xi}_a$ is the fluid particle displacement vector. Eliminating the condensation term from Eq. (4.3) and Eq. (4.8), the following relation is obtained

$$p = -B\nabla \cdot \vec{\xi}_a \tag{4.9}$$

The acoustic fluid is assumed to be inviscid, and the influence of thermal conductivity is ignored in order to construct the equation of dynamic equilibrium. Consider a fluid element $dV = dx\, dy\, dz$, which moves with the fluid and has a mass of *dm*. The net force $d\vec{f}$ on the element accelerates it according to the Newton's second law of motion. In the absence of viscosity, the element's net force along *x* direction is

$$df_x = \left[P - \left(P + \frac{\partial P}{\partial x} dx\right)\right] dy \rightleftarrows dz = -\frac{\partial P}{\partial x} dV \tag{4.10}$$

Thus, the total force on the fluid element is

$$d\vec{f} = -\nabla P dV \tag{4.11}$$

The acceleration of the fluid element is

$$\vec{a} = \frac{\partial \vec{u}_a}{\partial t} + \frac{\partial \vec{u}_a}{\partial x} u_{ax} + \frac{\partial \vec{u}_a}{\partial y} u_{ay} + \frac{\partial \vec{u}_a}{\partial z} u_{az} = \frac{\partial \vec{u}_a}{\partial t} + (\vec{u}_a \cdot \nabla)\vec{u}_a. \tag{4.12}$$

The mass of the fluid element is $dm = \rho\, dV$. Hence the force equation becomes

$$-\nabla P = \rho \left[\frac{\partial \vec{u}_a}{\partial t} + (\vec{u}_a \cdot \nabla)\vec{u}_a\right] \tag{4.13}$$

This nonlinear, inviscid force equation is referred to as the Euler's equation. However, since *s* is negligible and $|(\bar{u}_a \cdot \nabla)\vec{u}_a| << |\partial \vec{u}_a / \partial t|$, due to their low numeric values, therefore ρ can be replaced by ρ_o and the term $(\vec{u}_a \cdot \nabla)\vec{u}_a$ can be dropped, and the linear, inviscid force equation results as follows

$$\rho_o \frac{\partial \vec{u}_a}{\partial t} = -\nabla p \tag{4.14}$$

The equations of state (4.3), continuity (4.7), and force (4.14) can now be combined into a single differential equation with single dependent variable. The particle velocity can be omitted between Eq. (4.7) and Eq. (4.14). Taking the divergence of Eq. (4.14)

$$\rho_0 \nabla \cdot \frac{\partial \vec{u}_a}{\partial t} = -\nabla^2 p \tag{4.15}$$

Similarly, taking the time derivative of Eq. (4.7),

$$\frac{\partial^2 s}{\partial t^2} + \nabla \cdot \frac{\partial \vec{u}_a}{\partial t} = 0 \tag{4.16}$$

Eliminating $\vec{u}_a$ from these two relations produces

$$\nabla^2 p = \rho_o(\partial^2 s/\partial t^2). \tag{4.17}$$

Now the equation of state (4.3) is used to eliminate the condensation term from the equation above, whereby

$$\nabla^2 p = \frac{1}{c^2}\frac{\partial^2 p}{\partial t^2}; c = \left(\sqrt{B/\rho_o}\right) \tag{4.18}$$

This is the three-dimensional lossless wave equation. The one-dimensional equivalent of this equation, travelling along the *z*- direction, may be written as

$$\frac{\partial^2 p}{\partial z^2} = \frac{1}{c^2}\frac{\partial^2 p}{\partial t^2} \tag{4.19}$$

where $p = p(z,t)$. In the above equations, variable c is the speed of propagation of sound through the acoustic fluid medium. Any function, with argument $(ct \pm z)$, is a solution to Eq. (4.19). A solution, $f(ct - z)$ progresses towards the positive *z* direction, while the function $f(ct + z)$ advances in the negative *z* direction.

If it is now assumed that the medium is excited by a time-harmonic loading with a forcing frequency Ω such that

$$p(z,t) = p(z)\, exp(\, i\Omega t), u_a(z,t) = u_a(z)\, exp(i\Omega t) \tag{4.20}$$

then, equation (4.18) becomes

$$p_{,zz} - \frac{1}{c^2}\ddot{p} \equiv \left\{\frac{\partial^2 p(z)}{\partial z^2} + \frac{\Omega^2}{c^2}p(z)\right\}e^{i\Omega t} = 0 \tag{4.21}$$

Or, $\left(\frac{\partial^2 p}{\partial z^2}\right) + \frac{\Omega^2}{c^2}p = 0$ (4.22)

Or, $\left(\frac{\partial^2 p}{\partial z^2}\right) + k^2 p = 0$ (4.23)

Eq. (4.23) is the one-dimensional Helmholtz equation. The ratio k = Ω/*c*, is referred to as wavenumber.

The velocity (Neumann) boundary condition for the one-dimensional Helmholtz equation can be derived from the kinetic condition obtained from Eq. (4.14). The one-dimensional kinetic relation will be

$$\rho_o \frac{\partial \vec{u}_a}{\partial t} = -\frac{\partial p}{\partial z}.$$

By inserting relations (4.20) in it, the following relation is obtained:

$$\frac{\partial p(z)}{\partial z} e^{i\Omega t} = -\rho_o \frac{\partial}{\partial t}\left(u_a(z) e^{i\Omega t}\right)$$

Or, $\frac{\partial p(z)}{\partial z} e^{i\Omega t} = -i\Omega \rho_o u_a(z) e^{i\Omega t}$

Finally, eliminating the time variable, time, at boundary it is seen that

$$\frac{\partial p(z)}{\partial z} = -i\Omega \rho_o u_a(z) \qquad (4.24)$$

The three-dimensional Helmholtz equation is similarly derived and reads as follows

$$(\nabla^2 + k^2)p = 0 \qquad (4.25)$$

where ∇^2 is the Laplacian operator, given by

$$\nabla^2 = \frac{\partial^2}{\partial x^2} + \frac{\partial^2}{\partial y^2} + \frac{\partial^2}{\partial z^2} \qquad (4.26)$$

4.3 Numerical validation of two-dimensional acoustics problem

The acoustics medium is air at an ambient temperature of 20° Celsius at 1 atmosphere pressure. The speed of sound is assigned the value $c = 344 m/s$. The frequency chosen for the test is 400Hz. The velocity potential can be written as

$$\varphi(x, y) = \sin(\frac{k}{\sqrt{2}} x) \sin(\frac{k}{\sqrt{2}} y) \qquad (4.27)$$

where k is the wave number. If this solution is fed into equation (4.25), the equation is readily satisfied. Hence, this is evidently a solution for the Helmholtz equation. Now we will consider a two-dimensional acoustics problem whose boundary is detailed in figure 4.2 The boundary is considered as a square of side 0.1. The numbering of boundary nodes is given in anti-clockwise direction. We will take seven numbers of interior nodes each side so total forty-nine number of interior nodes. To understand mesh convergence study, we will first take eight numbers of boundary elements each side, then we will take sixteen, twenty-four and we will compare the interior nodes potential value between numerical and analytical solution.

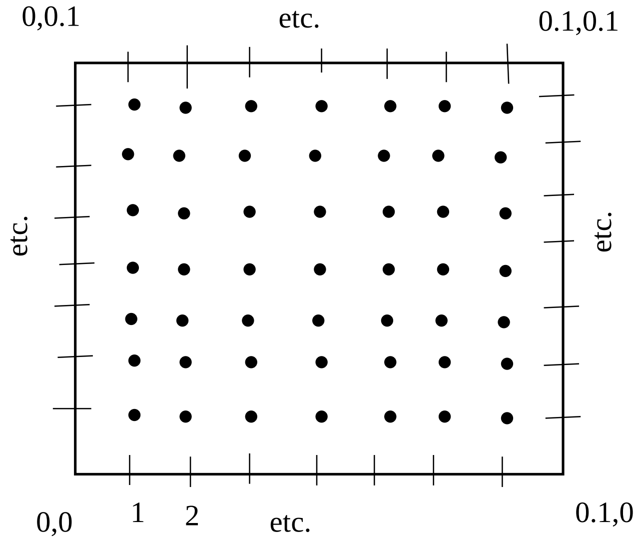

Figure 4.2: Numerical problem representation

$k =$ wave number $= \frac{2\times\pi\times400}{344}$=7.306029

Table 4.1: Output for the numerical problems and convergence study

Interior Node	x	y	Numerical values with N elements/side			Analytical results
			N=8	N=16	N=24	
1	0.0125	0.0125	0.00411	0.004156	0.004162	0.004164
2	0.0125	0.025	0.008292	0.008309	0.008311	0.008311
3	0.0125	0.0375	0.012419	0.012423	0.012424	0.012424
4	0.0125	0.05	0.016482	0.016484	0.016484	0.016484
5	0.0125	0.0625	0.020471	0.020476	0.020476	0.020476
6	0.0125	0.075	0.024353	0.024382	0.024383	0.024383
7	0.0125	0.0875	0.028171	0.028185	0.028187	0.028187
8	0.025	0.0125	0.008292	0.008309	0.008311	0.008311
9	0.025	0.025	0.016573	0.016587	0.016588	0.016588
10	0.025	0.0375	0.024788	0.024795	0.024796	0.024796
11	0.025	0.05	0.032896	0.0329	0.0329	0.0329
12	0.025	0.0625	0.040862	0.040867	0.040867	0.040867
13	0.025	0.075	0.048659	0.048663	0.048664	0.048664
14	0.025	0.0875	0.056275	0.056257	0.056257	0.056257
15	0.0375	0.0125	0.012419	0.012423	0.012424	0.012424
16	0.0375	0.025	0.024788	0.024795	0.024796	0.024796
17	0.0375	0.0375	0.037059	0.037064	0.037064	0.037064
18	0.0375	0.05	0.049176	0.049178	0.049178	0.049178
19	0.0375	0.0625	0.061087	0.061087	0.061087	0.061087
20	0.0375	0.075	0.072743	0.072742	0.072742	0.072742
21	0.0375	0.0875	0.084096	0.084093	0.084093	0.084093
22	0.05	0.0125	0.016482	0.016484	0.016484	0.016484
23	0.05	0.025	0.032896	0.0329	0.0329	0.0329
24	0.05	0.0375	0.049176	0.049178	0.049178	0.049178
25	0.05	0.05	0.065252	0.065252	0.065252	0.065252
26	0.05	0.0625	0.081056	0.081053	0.081053	0.081053
27	0.05	0.075	0.096521	0.096517	0.096517	0.096517
28	0.05	0.0875	0.111581	0.111578	0.111578	0.111578
29	0.0625	0.0125	0.020471	0.020476	0.020476	0.020476
30	0.0625	0.025	0.040862	0.040867	0.040867	0.040867
31	0.0625	0.0375	0.061087	0.061087	0.061087	0.061087
32	0.0625	0.05	0.081056	0.081053	0.081053	0.081053
33	0.0625	0.0625	0.100688	0.100682	0.100681	0.100681
34	0.0625	0.075	0.119901	0.11989	0.11989	0.119889
35	0.0625	0.0875	0.138606	0.138598	0.138598	0.138598
36	0.075	0.0125	0.024353	0.024382	0.024383	0.024383
37	0.075	0.025	0.048659	0.048663	0.048664	0.048664
38	0.075	0.0375	0.072743	0.072742	0.072742	0.072742
39	0.075	0.05	0.096521	0.096517	0.096517	0.096517
40	0.075	0.0625	0.119901	0.11989	0.11989	0.11989
41	0.075	0.075	0.142786	0.142764	0.142763	0.142762
42	0.075	0.0875	0.165072	0.165043	0.165041	0.16504
43	0.0875	0.0125	0.028171	0.028185	0.028187	0.028187
44	0.0875	0.025	0.056275	0.056257	0.056257	0.056257
45	0.0875	0.0375	0.084096	0.084093	0.084093	0.084093
46	0.0875	0.05	0.111581	0.111578	0.111578	0.111578
47	0.0875	0.0625	0.138606	0.138598	0.138598	0.138598
48	0.0875	0.075	0.165072	0.165043	0.165041	0.16504
49	0.0875	0.0875	0.190882	0.190806	0.190797	0.190794

Table 4.2: Error and Convergence study for increasing number of boundary elements

	% Error for Numerical values with N elements/side		
Interior Node	N=8	N=16	N=24
1	1.296829971	0.192122959	0.04803074
2	0.228612682	0.024064493	0
3	0.040244688	0.008048938	0
4	0.012132977	0	0
5	0.024418832	0	0
6	0.123036542	0.004101218	0
7	0.056763756	0.00709547	0
8	0.228612682	0.024064493	0
9	0.090426815	0.006028454	0
10	0.032263268	0.004032909	0
11	0.012158055	0	0
12	0.01223481	0	0
13	0.010274536	0.002054907	0
14	0.031996018	0	0
15	0.040244688	0.008048938	0
16	0.032263268	0.004032909	0
17	0.013490179	0	0
18	0.004066859	0	0
19	0	0	0
20	0.001374722	0	0
21	0.003567479	0	0
22	0.012132977	0	0
23	0.012158055	0	0
24	0.004066859	0	0
25	0	0	0
26	0.003701282	0	0
27	0.004144348	0	0
28	0.002688702	0	0
29	0.024418832	0	0
30	0.01223481	0	0
31	0	0	0
32	0.003701282	0	0
33	0.006952652	0.000993236	0
34	0.010009259	0.000834105	0.000834105
35	0.005772089	0	0
36	0.123036542	0.0041	0
37	0.010274536	0.002054907	0
38	0.001374722	0	0
39	0.004144348	0	0
40	0.009175077	0	0
41	0.016811196	0.001400933	0.000700467
42	0.019389239	0.001817741	0.000605914
43	0.056763756	0.00709547	0
44	0.031996018	0	0
45	0.003567479	0	0
46	0.002688702	0	0
47	0.005772089	0	0
48	0.019389239	0.001817741	0.000605914
49	0.046123044	0.006289506	0.001572376

Results and discussions

We are increasing number of the boundary elements from thirty-two to ninety-six. We can find out from the results in Tables 4.1 and 4.2 that with increasing the number of boundary elements, numerical results of interior nodes approach to analytical results. In case of 96 boundary elements (24 elements per side) solution is almost equal to exact analytical solution. So, increasing the number of meshes, numerical solution converges with analytical solution.

4.4 Case Study of Poisson's equation

Here we will try to solve a Poisson's equation problem using dual reciprocity boundary element method and try to compare with finite difference method (FDM). For this purpose, we take the following differential equation

$$\frac{\partial^2 u}{\partial x^2}+\frac{\partial^2 u}{\partial y^2}=-81xy \tag{4.28}$$

Subjected to following boundary conditions

For $0<x<1, 0<y<1$ given that $u(0,y)=0,\ u(x,0)=0, u(1,y)=100,\ u(x,1)=100$, we divide boundary into three parts. So, per part length $(h=1/3)$

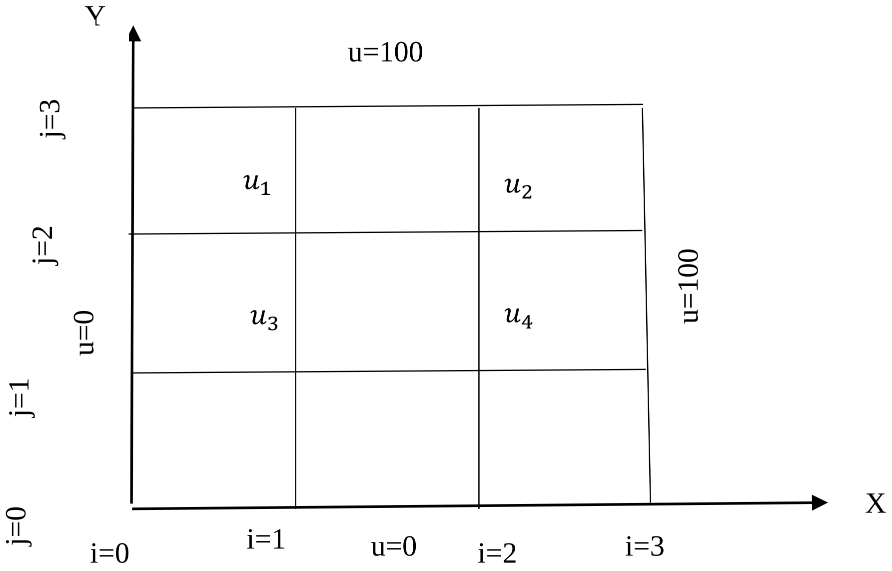

Figure 4.3: Mesh division of Poisson type problem

From standard five-point formula for Poisson equation

$$\frac{\partial^2 u}{\partial x^2}+\frac{\partial^2 u}{\partial y^2}=g(x,y) \tag{4.29}$$

Expression of $\frac{\partial^2 u}{\partial x^2},\frac{\partial^2 u}{\partial y^2}$ can be found from equations (A.42) and (A.43) respectively

$\frac{\partial^2 u}{\partial x^2}=\frac{u_{i-1,j}-2u_{i,j}+u_{i+1,j}}{h^2}$ and $\frac{\partial^2 u}{\partial y^2}=\frac{u_{i,j-1}-2u_{i,j}+u_{i,j+1}}{h^2}$ for square mesh neglecting higher order terms

Equation (4.29) can be written as (reference equation (A.46))

$$u_{i-1,j} + u_{i+1,j} + u_{i,j+1} + u_{i,j-1} - 4u_{i,j} = h^2 g(ih, jh) \qquad (4.30)$$

By applying (4.30) at each interior mesh point, we get linear equations in the nodal value $u_{i,j}$.

In our case, $h = 1/3$

The standard five-point formula for the above equation is

$$u_{i-1,j} + u_{i+1,j} + u_{i,j+1} + u_{i,j-1} - 4u_{i,j} = h^2 g(ih, jh) = h^2\big(-81(ih.jh)\big) = h^4(-81)ij = -ij \qquad (4.31)$$

For, u_1 $(i = 1, j = 2)$ equation (4.31) gives

$0 + u_2 + u_3 + 100 - 4u_1 = -2$

Or, $u_2 + u_3 - 4u_1 = -102$ (4.32)

For, u_2 $(i = 2, j = 2)$ equation (4.31) gives

$u_1 + 100 + u_4 + 100 - 4u_2 = -4$

Or, $u_1 + u_4 - 4u_2 = -204$ (4.33)

For, u_3 $(i = 1, j = 1)$ equation (4.31) gives

$0 + u_4 + 0 + u_1 - 4u_3 = -1$

Or, $u_4 + u_1 - 4u_3 = -1$ (4.34)

For, u_4 $(i = 2, j = 1)$ equation (4.31) gives

$u_3 + u_2 + 100 - 4u_4 = -2$

Or, $u_3 + u_2 - 4u_4 = -102$ (4.35)

After substituting (4.32) into equation (4.35) we get

$-4u_1 + 4u_4 = 0$

Or, $u_1 = u_4$ (4.36)

Then equation (4.33) becomes

$2u_1 - 4u_2 = -204$ (4.37)

And equation (4.34) becomes

$2u_1 - 4u_3 = -1$ (4.38)

Now, multiply equation (4.32) with 4 and add with equation (4.37) we get

$-14u_1 + 4u_3 = -612$ (4.39)

If we add equation (4.38) and equation (4.39)

$-12u_1 = -613$

Thus, $u_1 = 51.0833 = u_4$

From equation (4.4.9), we get

$u_2 = \frac{1}{2}(u_1 + 102) = 76.5477$

From equation (4.37) we get

$u_3 = \frac{1}{2}\left(u_1 + \frac{1}{2}\right) = 25.7916$

Table 4.3: Comparing FDM value with DRBEM values

Point	x	y	FDM value	DRM value	% Deviation from DRM
u1	0.33333	0.6667	51.0833	51.208457	0.244406896
u2	0.66667	0.6667	76.5477	78.060276	1.937702603
u3	0.33333	0.3333	25.7916	24.602019	4.835298274
u4	0.66667	0.3333	51.0833	51.208457	0.244406896

Table 4.4: Convergence study

	N elements/side in DRM						
Point	N=3	N=5	% Convergence	N=10	% Convergence	N=15	% Convergence
u1	51.208457	51.1812	0.05321679	51.17152	0.01896563	51.1699	0.00310339
u2	78.060276	77.8924	0.21551395	77.85023	0.054177104	77.8481	0.00274894
u3	24.602019	24.6955	0.37869591	24.70893	0.054194979	24.7095	0.00247273
u4	51.208457	51.1812	0.05321679	51.17152	0.018955857	51.1699	0.00311316

Results and Discussions

Here we have solved a Poisson type differential equation by using FDM and DRBEM, and compared them in Table 4.3. Initially we have taken a total of only twelve number of boundary elements and four internal nodes in DRBEM. Deviation from both the results is very small (within 5%). So, both the formulations are okay and acceptable. We have compared FDM results with a very crude mesh since we did hand computation. We cannot further refine the mesh in case of FDM since it will become increasingly difficult to carry out the hand computations. In Table 4.4 we studied convergence of results using only DRBEM by increasing gradually number of elements from 12 to 60 and we see that the error is decreasing monotonically.

Chapter 5

Conclusion

To solve any complicated engineering problem, computational methods are essential so as to consider difficult boundaries and boundary conditions. Various types of computational methods exist, namely, finite difference method, finite element method, and boundary element method. Among these methods, boundary element method asks for reduced input data, computation time and memory while proving same degree of accuracy.

Since a large class of engineering problems are governed by the generalized Helmholtz equations with variable coefficients, each of which could have separate fundamental solutions and separate codes, the Dual Reciprocity Boundary Element has been studied here that doesn't seek case-specific fundamental solutions and yet remains boundary only solution. Hence the same has been studied.

Two-dimension acoustics type problem has been solved here for validation. We know from previous discussions that sinusoidal acoustics is governed by a simple Helmholtz equation. Due to presence of non-homogeneous terms while solving Helmholtz type equation formulation, we bypass the domain integration using dual reciprocity principle and get boundary-only solution. We restricted ourselves to constant boundary elements.

Results show that though we have employed constant boundary elements, the domain potentials are very closely reproduced by the DRBEM in all validation problems. Potential values are also closely reproduced at the boundary, though the same is not true for the computed flux at the boundary in case of potential problems.

The internal potential solutions are very close to analytical results in case of DRBEM solution of Helmholtz equation.

Eventually, a Poisson equation is solved using the same program and the results are matched with a hand-computed finite difference solution of the same, along with mesh convergence study using DRBEM. It is observed that the for FDM results with crude mesh deviation of results by DRBEM is within 5% at the most. Next the elements are rendered finer to conduct a mesh convergence study and observed that the results manifest a monotonic convergence.

APPENDIX-A

(Derivation of mathematical expressions)

A.1) Transformation of Laplace equation in Polar Coordinates

$$\frac{\partial^2\varphi}{\partial x^2}+\frac{\partial^2\varphi}{\partial y^2}=0$$

φ is the function of (x,y)

If we use polar coordinates (r,θ) whose center is (0,0) defined by

$y=r\sin\theta$ and $x=r\cos\theta$
Then if we can introduce $\psi(r,\theta)=\varphi(r\cos\theta\,,r\sin\theta)$

$r=\sqrt{x^2+y^2}$ and $\theta=tan^{-1}({}^{y}\!/_{x})$

$$\frac{\partial r}{\partial x}=\frac{x}{\sqrt{x^2+y^2}}=\cos\theta$$

$$\frac{\partial\theta}{\partial x}=-\frac{y}{\sqrt{x^2+y^2}}=-\frac{\sin\theta}{r}$$

$$\frac{\partial u}{\partial x}=\frac{\partial u}{\partial r}.\frac{\partial r}{\partial x}+\frac{\partial u}{\partial\theta}.\frac{\partial\theta}{\partial x}=\cos\theta\ \frac{\partial u}{\partial r}-\frac{\sin\theta}{r}\frac{\partial u}{\partial\theta}$$

$$\frac{\partial}{\partial x}=\cos\theta\ \frac{\partial}{\partial r}-\frac{\sin\theta}{r}\frac{\partial}{\partial\theta}$$

Similarly, $\frac{\partial}{\partial y}=\sin\theta\ \frac{\partial}{\partial r}+\frac{\cos\theta}{r}\frac{\partial}{\partial\theta}$

$$\frac{\partial^2u}{\partial x^2}=\frac{\partial}{\partial x}\left(\frac{\partial u}{\partial x}\right)=(\cos\theta\ \frac{\partial}{\partial r}-\frac{\sin\theta}{r}\frac{\partial}{\partial\theta})(\cos\theta\ \frac{\partial u}{\partial r}-\frac{\sin\theta}{r}\frac{\partial u}{\partial\theta})$$

$$=\cos^2\theta\ \frac{\partial^2u}{\partial r^2}-\frac{2\sin\theta\cos\theta}{r}\frac{\partial^2u}{\partial r\partial\theta}+\frac{\sin^2\theta}{r^2}\frac{\partial^2u}{\partial\theta^2}+\frac{\sin^2\theta}{r}\frac{\partial u}{\partial r}+\frac{2\sin\theta\ \cos\theta}{r^2}\frac{\partial u}{\partial\theta}\qquad\text{(A.1)}$$

Similarly,

$$\frac{\partial^2u}{\partial y^2}=\frac{\partial}{\partial y}\left(\frac{\partial u}{\partial y}\right)=(\sin\theta\ \frac{\partial}{\partial r}+\frac{\cos\theta}{r}\frac{\partial}{\partial\theta})(\sin\theta\ \frac{\partial u}{\partial r}-\frac{\cos\theta}{r}\frac{\partial u}{\partial\theta})$$

$$=\sin^2\theta\ \frac{\partial^2u}{\partial r^2}+\frac{2\sin\theta\cos\theta}{r}\frac{\partial^2u}{\partial r\partial\theta}+\frac{\cos^2\theta}{r^2}\frac{\partial^2u}{\partial\theta^2}+\frac{\cos^2\theta}{r}\frac{\partial u}{\partial r}-\frac{2\sin\theta\ \cos\theta}{r^2}\frac{\partial u}{\partial r}\qquad\text{(A.2)}$$

Adding equation (1a) and (2a) we get

$$\frac{\partial^2u}{\partial x^2}+\frac{\partial^2u}{\partial y^2}=\frac{\partial^2u}{\partial r^2}+\frac{1}{r^2}\frac{\partial^2u}{\partial\theta^2}+\frac{1}{r}\frac{\partial u}{\partial r}$$

$$\frac{1}{r}\frac{\partial}{\partial r}\left(r\frac{\partial\psi}{\partial r}\right)+\frac{1}{r^2}\frac{\partial^2\psi}{\partial\theta^2}=0\qquad\text{(A.3)}$$

A.2) Gauss-Green Theorem

Gauss-Green theorem which is a fundamental theorem relating the integral of the derivative of a function across a domain R with the function's integral on the boundary C. Theorem can be applicable two-dimensional or three-dimensional domain. Here for the sake of simplicity for two-dimensional instance relationship is derived. Let us consider the plane domain R which is confined by the curve C. Consider the derivative with respect to x of a function $f=f(x,y)$.

The integration over R can be expressed in the form of double integral, in which the integration is performed with respect to x first, then with respect to y. So, it can be written

$$\int_{\mathrm{R}} \frac{\partial f}{\partial x}\, dR = \int_{y_1}^{y_2}\left(\int_{x_1}^{x_2} \frac{\partial f}{\partial x}\, dx\right)dy = \int_{y_1}^{y_2}\{f(x_2\,,y) - f(x_1,y)\}dy \tag{A.4}$$

Where

$$x_1 = x_1(y) \text{ and } x_2 = x_2(y) \tag{A.5}$$

From figure (A-1, A-2) we have

$$\left(\frac{dy}{ds}\right) = \cos\alpha = n_x$$

$$\text{or, } dy = n_x\, ds \tag{A.6}$$

$$-\left(\frac{dx}{ds}\right) = \sin\alpha = n_y$$

$$\text{Or, } dx = -\,n_y\, ds \tag{A.7}$$

n_x, n_y are the components of the unit vector **n**, perpendicular to the boundary C . When the angle α is measured in anti-clockwise direction with regard to the positive x-direction dx and $\sin\alpha$ are opposite signs (Reference figure A-1)

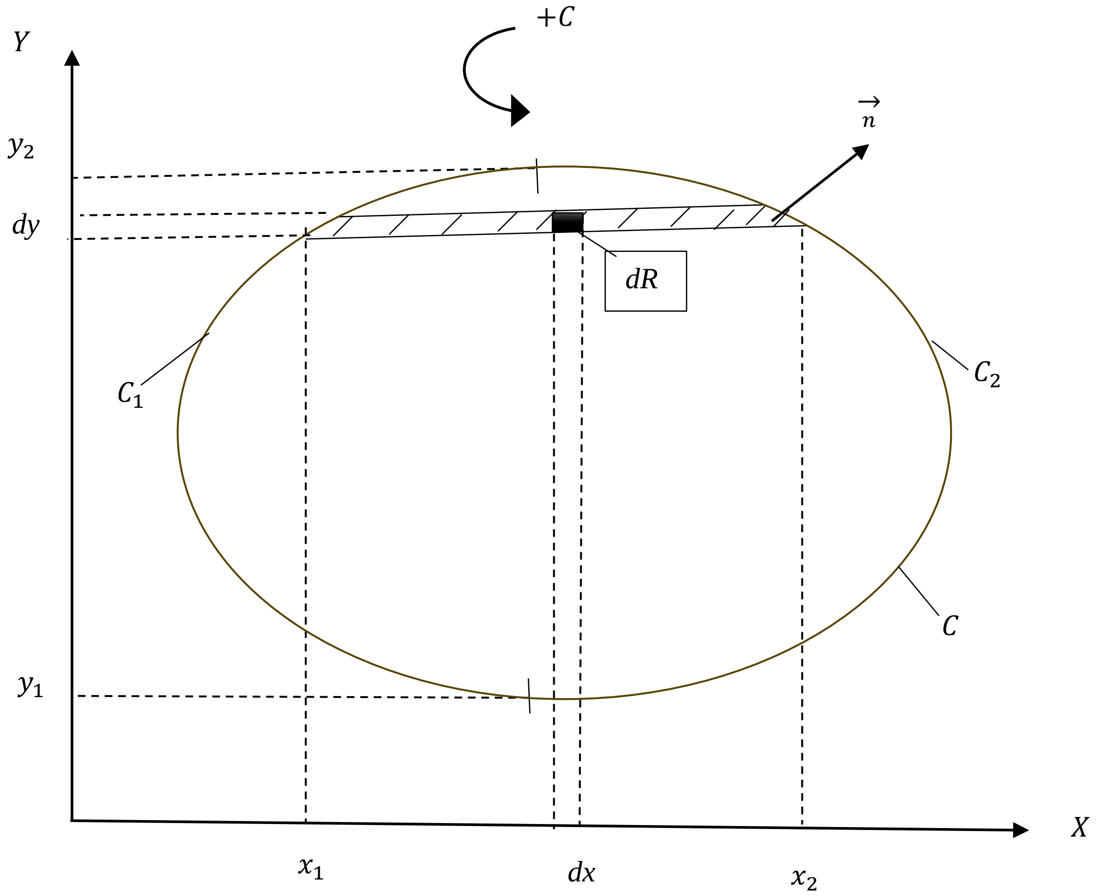

Figure A-1: Problem domain definition for Gauss Green theorem

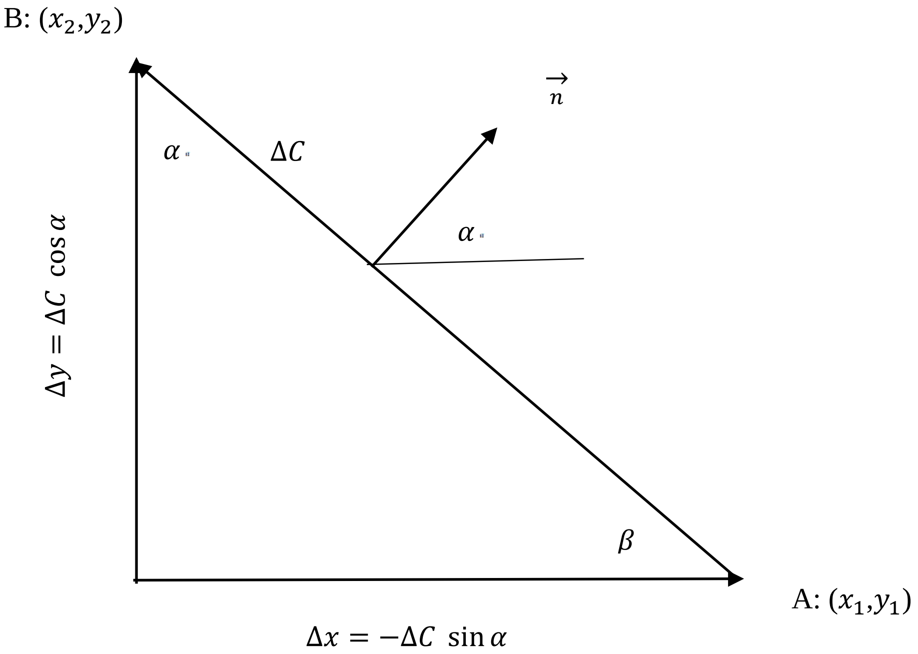

Figure A-2: Surface element definition

$$\int_{y_1}^{y_2}\{f(x_2,y)-f(x_1,y)\}dy = \int_{s_2} f(x_2,y)n_x ds - \int_{s_1} f(x_1,y)n_x ds \qquad \text{(A.8)}$$

When y changes from y_1 and y_2 the integration on s_1 is conducted in the clockwise direction (negative direction) in the above expression. We can write the above equation in combined form

$$\int_{\mathrm{R}} \frac{\partial f}{\partial x} dR = \int_{\mathrm{C}} f n_x ds \qquad \text{(A.9)}$$

Interchanging x with y in equation (A.9), we can get

$$\int_{\mathrm{R}} \frac{\partial f}{\partial y} dR = \int_{\mathrm{C}} f n_y ds \qquad \text{(A.10)}$$

If g is another function of x, y then from equations (A.9) and (A.10) we obtain

$$\int_{\mathrm{R}} \frac{\partial (fg)}{\partial x} dR = \int_{\mathrm{C}} fgn_x\, ds = \int_{\mathrm{R}} g\frac{\partial f}{\partial x} dR + \int_{\mathrm{R}} f\frac{\partial g}{\partial x} dR$$

$$\int_{\mathrm{R}} g\frac{\partial f}{\partial x} dR = -\int_{\mathrm{R}} f\frac{\partial g}{\partial x} dR + \int_{\mathrm{C}} fgn_x ds \qquad \text{(A.11)}$$

$$\int_{\mathrm{R}} \frac{\partial (fg)}{\partial y} \mathrm{dR} = \int_{\mathrm{C}} fgn_y\, ds = \int_{\mathrm{R}} g\frac{\partial f}{\partial y} \mathrm{dR} + \int_{\mathrm{R}} f\frac{\partial g}{\partial y} \mathrm{dR} \qquad \text{(A.12)}$$

$$\int_{\mathrm{R}} g\frac{\partial f}{\partial y} dR = -\int_{\mathrm{R}} f\frac{\partial g}{\partial y} dR + \int_{\mathrm{C}} fgn_y ds$$

Equations (A.11) and (A.12) states integration by parts in two dimensions and termed as *Gauss-Green theorem.*

A.3) Gauss divergence theorem

It is Gauss-Green theorem's application. Consider a vector field $= u\mathbf{i} + v\mathbf{j}$ **,** where **i**, **j** is the unit vector along x and y axes, respectively. its components are $u = u(x, y), v = v(x, y)$. Apply equations (A.9) and (A.10) to $f = u$ and $f = v$ respectively, then after addition we can get,

$$\int_{\mathrm{R}} (\frac{\partial u}{\partial x} + \frac{\partial v}{\partial y})dR = \int_{\mathrm{C}} (u n_x + v n_y)ds \qquad \text{(A.13)}$$

If the coordinates x and y are represented by x_1 and x_2, respectively, then vector field $\boldsymbol{u}$ components can be represented by u_i $(i = 1{,}2)$ and those of the normal vector $\boldsymbol{n}$ by n_i. Therefore, we can write equation (13.a) as

$$\int_{\mathrm{R}} (\frac{\partial u_1}{\partial x_1} + \frac{\partial u_2}{\partial x_2})dR = \int_{\mathrm{C}} (u_1 n_1 + u_2 n_2)ds \qquad \text{(A.14)}$$

We can write in summation convention

$$\int_{\mathrm{R}} \frac{\partial u_i}{\partial x_i} dR = \int_{\mathrm{C}} u_i n_i ds \qquad (i = 1{,}2) \qquad \text{(A.15)}$$

Equations (2.9) to (2.11) can be written using vector notation as

$$\int_{\mathrm{R}} \nabla.\boldsymbol{u}\, dR = \int_{\mathrm{C}} \boldsymbol{u}.\boldsymbol{n}\, ds \qquad \text{(A.16)}$$

Symbolic vector ∇ can be defined as

$$\nabla \equiv \mathbf{i}\frac{\partial}{\partial \mathrm{x}} + \mathbf{j}\frac{\partial}{\partial \mathrm{y}} = \boldsymbol{i_1}\frac{\partial}{\partial x_1} + \boldsymbol{i_2}\frac{\partial}{\partial x_2} \qquad \text{(A.17)}$$

It denotes the differential operator that generates a scalar field's gradient.

The dot product between the vectors ∇ and u that is $\nabla.\mathbf{u}$ is termed as divergence of a vector field u at a point inside the domain R, whereas the quantity $\boldsymbol{u}.\boldsymbol{n}$ is termed as flux at a point on the boundary C. The projection of $\boldsymbol{u}$ in the direction of $\boldsymbol{n}$ is expressed by dot product. The Gauss divergence theorem connects the total divergence to the total flux of a vector field (equation A.16).

A.4) Green's second identity

Now if we assume two functions $u = u(x, y)$ and $v = v(x, y)$, which are twice continuously differentiable in domain R and once on C. Now we apply equation (11.a) for $g = v, f = \frac{\partial u}{\partial y}$ after addition the resulting equations we get

$$\int_{\mathrm{R}} v(\frac{\partial^2 u}{\partial x^2} + \frac{\partial^2 u}{\partial y^2})dR = -\int_{\mathrm{R}} (\frac{\partial u}{\partial x}\frac{\partial v}{\partial x} + \frac{\partial u}{\partial y}\frac{\partial v}{\partial y})dR + \int_{\mathrm{C}} v(\frac{\partial u}{\partial x}n_x + \frac{\partial u}{\partial y}n_y)ds$$

(A.18)

Similarly, we apply equation (A.11) for $g = u, f = \frac{\partial v}{\partial x}$ and equation (A.12) for $g = u, f = \frac{\partial v}{\partial y}$ and after addition we can get

$$\int_{\mathrm{R}} u(\frac{\partial^2 v}{\partial x^2} + \frac{\partial^2 v}{\partial y^2})dR = -\int_{\mathrm{R}} (\frac{\partial u}{\partial x}\frac{\partial v}{\partial x} + \frac{\partial u}{\partial y}\frac{\partial v}{\partial y})dR + \int_{\mathrm{C}} u(\frac{\partial v}{\partial x}n_x + \frac{\partial v}{\partial y}n_y)ds$$

(A.19)

Now we subtract equation (A.18) from equation (A.19) and we get

$$\int_{\mathrm{R}} (v\nabla^2 u - u\nabla^2 v)dR = \int_{\mathrm{C}} (v\frac{\partial u}{\partial n} - u\frac{\partial v}{\partial n})ds \tag{A.20}$$

∇^2 is termed as *Laplace operator* and it is defined as

$$\nabla^2 \equiv \nabla.\nabla = \left(\mathbf{i}\frac{\partial}{\partial \mathrm{x}} + \mathbf{j}\frac{\partial}{\partial \mathrm{y}}\right).\left(\mathbf{i}\frac{\partial}{\partial \mathrm{x}} + \mathbf{j}\frac{\partial}{\partial \mathrm{y}}\right) = \frac{\partial^2}{\partial \mathrm{x}^2} + \frac{\partial^2}{\partial \mathrm{y}^2} \tag{A.21}$$

While

$$\frac{\partial}{\partial n} \equiv n.\nabla = (n_x i + n_y j).\left(\mathbf{i}\frac{\partial}{\partial \mathrm{x}} + \mathbf{j}\frac{\partial}{\partial \mathrm{y}}\right) = n_x\frac{\partial}{\partial \mathrm{x}} + n_y\frac{\partial}{\partial \mathrm{y}} \tag{A.22}$$

Equation (A.20) is termed as *Green's second identity* for the harmonic operator or *Green's reciprocal identity.*

A.5) The Dirac Delta function

In mechanics problems concentrated loads applied to a very small region theoretically a point or an instant of time. These problems can be expressed as Dirac delta function. We have used some of Dirac delta functions property for the development of boundary element formulation

Dirac delta function can be written as $\delta(x)$. The one-dimensional Dirac-delta function defined by following relations

$$\delta(x) = \begin{cases} 0, & x \neq 0 \\ \infty, & x = 0 \end{cases} \tag{A.23}$$

$$\int_{-\infty}^{+\infty} \delta(x)\, dx = \int_{-\epsilon}^{\epsilon} \delta(x)\, dx = 1 \tag{A.24}$$

Where ϵ is a very small positive real number. According to the definition, the Dirac delta function has zero value everywhere except at point $x = 0$, where its value is infinite.

The one-dimensional Dirac delta function is defined by the relation

$$\int_{-\infty}^{+\infty} \delta(x)\, h(x)\, dx = h(0) \tag{A.25}$$

For a point source applied at the position $x = 0$ or by relation

$$\int_{-\infty}^{+\infty} \delta(x - x_0)\, h(x)\, dx = h(x_0) \tag{A.26}$$

The Dirac delta function $\delta(Q - Q_0)$ in two dimensions can be defined as

$$\int_{\mathrm{R}} \delta(Q - Q_0)\, h(Q)\, dR_Q = h(Q_0)\,,\ \ Q(x, y),\ \ \ Q_0(x_0, y_0) \in \mathrm{R} \tag{A.27}$$

For an arbitrary function h(Q), which is continuous in the domain R the point $Q_0(x_0, y_0)$ is in it the two-dimensional Dirac delta can be written as

$$\delta(Q - Q_0) = \begin{cases} 0, & Q \neq Q_0 \\ \infty, & Q = Q_0 \end{cases} \tag{A.28}$$

$$\int_{\mathrm{R}} \delta(Q - Q_0)\ dR_Q = 1\ ,\ \ Q_0(x_0, y_0) \in \mathrm{R} \tag{A.29}$$

A.6) Representation of r

Let us, say that points within the domain R are designated by upper case letters such as $P(x, y)$ whereas boundary points are denoted by lower case letters example $q(\xi, \eta)$. The angle between x-axis and the vector r is indicated by α and the angle between x-axis and the unit vector $\boldsymbol{n}$ normal to the boundary q is by β (reference figure A-3). We may define the angle θ using these two angles as

$$\theta = angle(r, n) = \beta - \alpha \tag{A.30}$$

To derive the expression $\frac{\partial \varphi_1}{\partial n}$

Refer to below fig A-3, it is

$$\cos\alpha = \frac{x - \xi}{r}$$

$$\sin\alpha = \frac{y - \eta}{r}$$

$$r = |q - P| = \sqrt{(x - \xi)^2 + (y - \eta)^2} \tag{A.31}$$

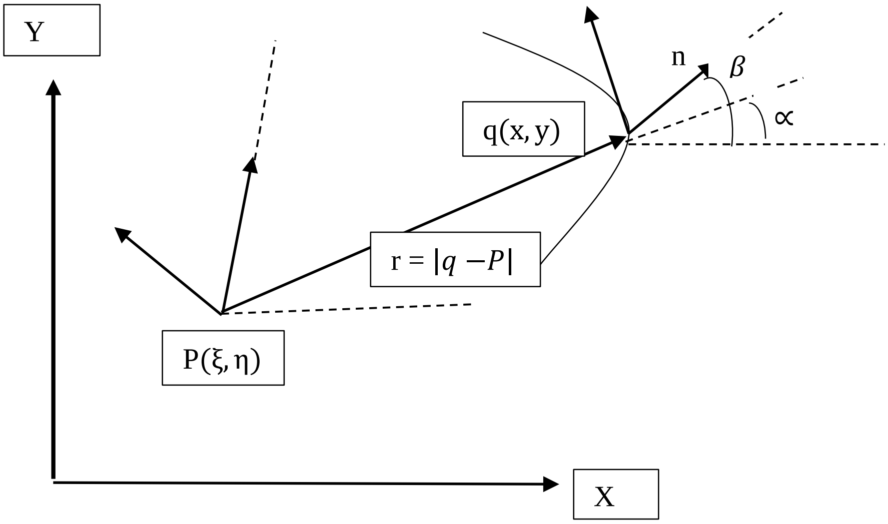

Figure A-3: Definitions in geometric form relating the relative location of field point and boundary point

Now, $\frac{\partial r}{\partial x} = \frac{\partial\sqrt{(x-\xi)^2+(y-\eta)^2}}{\partial(x-\xi)^2+(y-\eta)^2} . \frac{\partial(x-\xi)^2+(y-\eta)^2}{\partial x} = \frac{1}{2}((x-\xi)^2+(y-\eta)^2)^{(-\frac{1}{2})}.[-2(x-\xi)]$

Hence, $\frac{\partial r}{\partial x} = -\frac{x-\xi}{r} = -\cos\alpha$ (A.32)

Again, $\frac{\partial r}{\partial \xi} = \frac{\partial\sqrt{(x-\xi)^2+(y-\eta)^2}}{\partial(x-\xi)^2+(y-\eta)^2} . \frac{\partial(x-\xi)^2+(y-\eta)^2}{\partial \xi} = \frac{1}{2}((x-\xi)^2+(y-\eta)^2)^{(-\frac{1}{2})}.2(x-\xi)$;

Hence, $\frac{\partial r}{\partial \xi} = \frac{x-\xi}{r} = \cos\alpha$ (A.33)

$$\frac{\partial r}{\partial y} = \frac{\partial\sqrt{(x-\xi)^2+(y-\eta)^2}}{\partial(x-\xi)^2+(y-\eta)^2} . \frac{\partial(x-\xi)^2+(y-\eta)^2}{\partial y} = \frac{1}{2}((x-\xi)^2+(y-\eta)^2)^{(-\frac{1}{2})}.[-2(y-\eta)]$$

$$\frac{\partial r}{\partial y} = -\frac{y-\eta}{r} = -\sin\alpha \quad (A.34)$$

$$\frac{\partial r}{\partial \eta} = \frac{\partial\sqrt{(x-\xi)^2+(y-\eta)^2}}{\partial(x-\xi)^2+(y-\eta)^2} . \frac{\partial(x-\xi)^2+(y-\eta)^2}{\partial \eta} = \frac{1}{2}((x-\xi)^2+(y-\eta)^2)^{(-\frac{1}{2})}.2(y-\eta)$$

Hence, $\frac{\partial r}{\partial \eta} = \frac{y-\eta}{r} = \sin\alpha$ (A.35)

We know from figure A-3 that,

$\cos\beta = n_x$ and $\sin\beta = n_y$ (A.36)

Now we apply chain rule of expanding a derivative

$$\frac{\partial r}{\partial n} = \frac{\partial r}{\partial x}\frac{\partial x}{\partial n} + \frac{\partial r}{\partial y}\frac{\partial y}{\partial x} = \frac{\partial r}{\partial x}\cos\beta + \frac{\partial r}{\partial y}\sin\beta = r_{,x}\, n_x + r_{,y} n_y$$

If we substitute term from equations (A.32) to (A.36) by term then we get

Or, $\frac{\partial r}{\partial n} = \cos\alpha\cos\beta + \sin\alpha\sin\beta = \cos(\beta-\alpha) = \cos\theta$ (A.37)

Hence, $\frac{\partial \varphi_1}{\partial n} = \frac{\partial \varphi_1}{\partial r}\frac{\partial r}{\partial n} = \frac{1}{2\pi}\frac{1}{r}\cos\theta = \frac{\cos\theta}{2\pi r}$ (A.38)

A.7) Numerical formulation of Finite Difference Method (FDM)

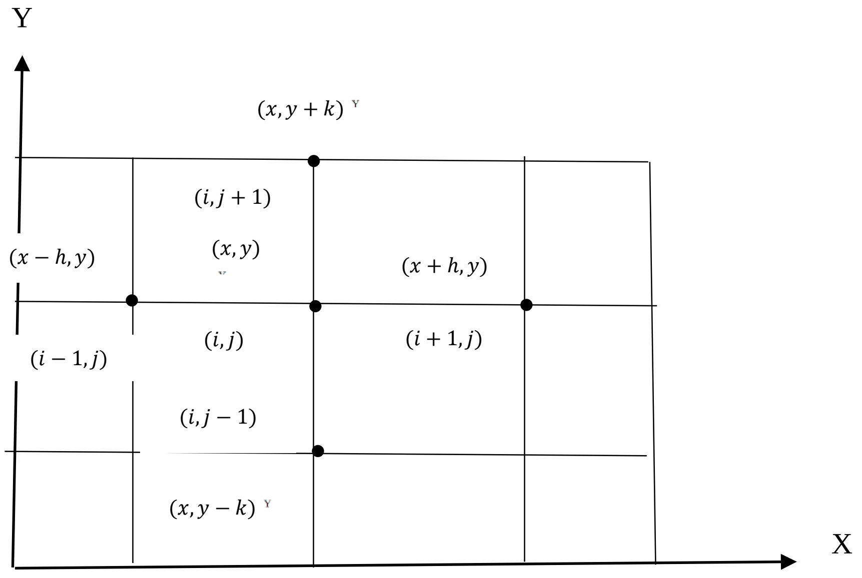

Figure A-4: Mesh division for finite difference method

We consider a rectangular region R in the plane x, y. We can divide the entire region into a rectangular network of sides $\Delta x = h\ and\ \Delta y = k$ as shown in **figure A-4 .** The intersection points are called mesh points.

Using Taylor's series expansion, we can write

$$u_{i+1,j} = u(x+h, y) = u(x, y) + h\frac{\partial u(x,y)}{\partial x} + \frac{h^2}{2}\frac{\partial^2 u(x,y)}{\partial x^2} + \frac{h^3}{6}\frac{\partial^3 u(x,y)}{\partial x^3} + \cdots \qquad \text{(A.39)}$$

Similarly,

$$u_{i-1,j} = u(x-h, y) = u(x, y) - h\frac{\partial u(x,y)}{\partial x} + \frac{h^2}{2}\frac{\partial^2 u(x,y)}{\partial x^2} - \frac{h^3}{6}\frac{\partial^3 u(x,y)}{\partial x^3} + \cdots \qquad \text{(A.40)}$$

Adding equation (A.39) and equation (A.40) we get

$$\frac{\partial^2 u(x,y)}{\partial x^2} = \frac{u(x+h,y) - 2u(x,y) + u(x-h,y)}{h^2} + O(h^2) \qquad \text{(A.41)}$$

$O(h^2)$ is dominant error which is a function of h^2

Or, we can write equation (c) as below

$$u_{xx} = \frac{u_{i-1,j} - 2u_{i,j} + u_{i+1,j}}{h^2} + O(h^2) \qquad \text{(A.42)}$$

Similarly, we can write in Y direction

$$u_{yy} = \frac{u_{i,j-1} - 2u_{i,j} + u_{i,j+1}}{k^2} + O(k^2) \qquad \text{(A.43)}$$

If we consider square grid then $h = k$ and we add equation (A.42) and equation (A.43) neglecting higher order error terms we will get

$$u_{xx} + u_{yy} = \frac{u_{i-1,j} - 2u_{i,j} + u_{i+1,j}}{h^2} + \frac{u_{i,j-1} - 2u_{i,j} + u_{i,j+1}}{h^2} \qquad \text{(A.44)}$$

In case of Poisson equation

$$\frac{\partial^2 u}{\partial x^2} + \frac{\partial^2 u}{\partial y^2} = g(x, y) \qquad \text{(A.45)}$$

Put equation (A.44) into equation (A.45) we get

$$\frac{u_{i-1,j} - 2u_{i,j} + u_{i+1,j}}{h^2} + \frac{u_{i,j-1} - 2u_{i,j} + u_{i,j+1}}{h^2} = g(x, y)$$

Or, $u_{i-1,j} - 2u_{i,j} + u_{i+1,j} + u_{i,j-1} - 2u_{i,j} + u_{i,j+1} = h^2 g(x, y)$

Or, $u_{i-1,j} + u_{i+1,j} + u_{i,j-1} + u_{i,j+1} - 4u_{i,j} = h^2 g(x, y)$ (A.46)

References

[1] Green G. An essay on the application on mathematical analysis to the theories of electricity and magnetism, T. Wheelhouse: Nottingham; 1828

[2] Betti E. Theoria dell' Elasticita`. Il Nuovo Cimento 1872;6-10, Ser. 2

[3] Somigliana C. Sopra l' Equilibrio di' un Corpo Elastico Isotropo. Il Nuovo Cimento 1875;18(1):91-6 Ser. 3

[4] Fredholm I. Sur une classe d' equations fonctionelles. Acta Mathematica 1903; 27:365-90

[5] Jaswon MA. Integral equation methods in potential theory I. Proc R Soc Ser A 1963; 275:23-32

[6] Symm GT. Integral equation methods in potential theory II. Proc R Soc Ser A 1963; 275:33-46.

[7] Jaswon M. and Pointer,A.R. An Integral equation solution of the Torsion Problem. Proc Roy, Soc Ser A 1963;273:237-246

[8] Hess, 1. L., and Smith, A M. 0., Calculation of potential flow about arbitrary bodies, Progress in Aeronautical Sciences Vol. 8, (D. Kiichemann, Ed.), Pergamon Press, London, 1967.

[9] Cruse, T.A. and Rizzo F.J., A direct formulation and numerical solution of the general transient elasto-dynamic problem, I,J. Math. Anal. Appl. 22, 244-259 (1968)

[10] Nardini D, Brebbia CA. New approach to free vibration analysis using boundary elements. In: Brebbia CA, editor. Boundary element methods in engineering. Southampton and Boston: Springer-Verlag, Berlin and Computational Mechanics Publications; 1982. p. 312_26.

[11] Wrobel, L.C., Brebbia, C.A. and Nardini, D. (1986). The dual reciprocity boundary element formulation for transient heat conduction. *Finite elements in Water resources VI,* Computational Mechanics Publications, Southampton and Springer-Verlag, Berlin and New York.

[12]Partridge, P.W. and Brebbia, C.A. (1990a). Computational implementation of the BEM dual reciprocity method for the solution of general field equations, Communications in Applied Numerical Methods, Vol.6, 83-92.

[13] Ang W.T.,2007, A Beginner's Course in Boundary Element Methods, Universal-Publishers, 2007.

[14] Brebbia C.A., Dominguez J., Boundary Elements an Introductory Course, WIT Press, 1998

[15] Katsikadelis J.T., The Boundary Element Method for Engineers and Scientists Theory and Applications, Elseier, 2nd edition,2002

[16] Loeffler, C.F. and Mansur, W.J. 'Dual reciprocity boundary element formulation for potential problems in infinite domains', Boundary Elements X, Vol .2, Ed. C.A. Brebbia, Computational Mechanics Publications, Springer-Verlag, 1988.

[17] Zhu, S. and Zhang, Y. (1992b). Solving general field equations in infinite domains with dual reciprocity boundary element method. *Engineering Analysis with Boundary Elements* (in press).

[18] Zhu, S. and Zhang, Y. (1993). A new approach to exterior problems with the dual reciprocity method. *Boundary Elements XV*, Brebbia, C.A. and Conner, J.J.

(eds.), pp. 359-373, Computational Mechanics Publication and Elsevier Applied Science.

[19] Jumarhon, B., Amini, S. and Chen, Ke (1998). On the boundary element dual reciprocity method. , Elsevier Science Ltd, Great Britain.

[20] Marin, L., Elliot, L., Heggs, P.J., Ingham, D.B, Lesnic, D., Wen. X . Dual reciprocity boundary element method solution of the Cauchy problem for Helmholtz- type equations with variable coefficients,Elsevier, Journal of sound and vibration.

[21] Mersenne, Marin. 1636. *Harmonie universelle*. Paris: S. Cramoisy; English translation: Hawkins, J. 1853. *General History of the Practice and Science of Music*. London: J. A. Novello, pp. 600–616, 650 ff.

[22] Galileo, Galilei. 1638 (translation published in 1939). *Dialogues Concerning Two New Sciences*, Translated by Crew, H. and De Salvio, A. Evanston, IL: Northwestern University Press.

[23] Chladni, E. F. F. 1802. *Die Acustik*. Leipzig: Breitkopf & Hartel

[24] Newton, Sir Isaac. 1687. *Philosophiae Naturalis Principia Mathematica*. London: Joseph Streater for the Royal Society.
[25] Sabine, W.,1922, Harvard University Press; republished, Acoustical Society of America, 1993

[26] Kirkup,S.M., Amini.S., Solution of the Helmholtz eigen value problem via the boundary element method, International journal for numerical methods in engineering,1993.

[27] Kirkup, S.M., Jones, M.A., Computational Methods for acoustic Modal Analysis of an Enclosed Fluid With Application to a Loudspeaker Cabinet, Applied Acoustics, Elsevier SCIENCE ltd,1996.

[28] Amini, S., Kirkup, S.M., Solution of Helmholtz Equation in the Exterior Domain by Elementary Boundary Integral Methods, Journal of computational physics 118,208-221, 1995

[29] Kirkup, S., Solution of exterior acoustic problems by the boundary element method, 1989

[30] Kirkup, S., The Boundary Element Method in Acoustics: A Survey, Applied Science, 2019

[31] Kirkup, S., The Boundary Element Method in Acoustics, book in Journal of Computational Acoustics, 2007

[32] Raichel, D.R., The science and applications of acoustics, second edition, Springer publication

[33] Kinsler, L.E., Frey, A.R., Coppens, A.B., Sanders, J.V., Fundamental of Acoustics, 4th edition, John Wiley & Sons, Inc.

[34] Baby, A. *et al.*,2021, Building Acoustics in Civil Engineering, International Journal of Science, Engineering and Technology.

[35] Drozdek. J., Majchrzak. E., NUMERICAL SOLUTION OF BIOHEAT TRANSFER EQUATION BY MEANS OF THE DUAL RECIPROCITY BEM, Scientific Research of the Institute of Mathematics and Computer Science, May 2007

[36] Pennes, H.H., Analysis of Tissue and Arterial Blood Temperatures in the Resting Human Forearm Journal of APPLIED PHYSIOLOGY Vol I AUGUST 1948 Number 2

[37] Gumerov, N.A., Duraiswami, R., Fast Multipole Methods for the Helmholtz Equation in Three Dimensions-Elsevier Science (2005), Elsevier Series in Electromagnetism.